JNC TN9400 2002-037

Analysis Results on BFS-62-3A Experiment Using IPPE Standard System

June 2002

O-ARAI ENGINEERING CENTER
JAPAN NUCLEAR CYCLE DEVELOPMENT INSTITUTE

JNC TN9400 2002-037
June 2002

Analysis Results on BFS-62-3A Experiment Using IPPE Standard System

Mikhail SEMENOV *)

ABSTRACT

This report is devoted to analysis of experimental studies performed on BFS-62-3A critical assembly in Russia. The objective of work is verification of the TRIGEX code for reactor neutronics analysis as applied to the hybrid core of the BN-600 reactor of Beloyarskaya NPP.

Calculation models are described in the report, and results of analysis are compared with experimental data. The analysis was made by using the TRIGEX code mainly. FFCP code was used for taking into account heterogeneous structure of the BFS fuel regions. This code was coupled with the TRIGEX code for preparing averaged macro and micro cross-sections. Also, in the report, results of Monte-Carlo calculations with MMKKENO code are described. These calculations were used; first of all, for definition "reference" criticality and for confirming of correction values obtained with deterministic codes. The ABBN-93 system with the constant preparation CONSYST code was used as cross-section base.

The following parameters were analyzed: criticality, control rod worth, sodium void reactivity effect, fission rate distribution and central reaction cross-section ratios (spectral indices).

On the average, the differences between analytical results based on TRIGEX code calculations and experimental data do not exceed the following values:

- **0.1**%$\Delta k/k$ - for k_{eff},
- **6**% - for control rod worth,
- **4**% - for fission rate distribution within the core,
- **0.2** pcm/kg – for sodium void reactivity effect

This work is related to the JNC-IPPE Collaboration on Experimental Investigation of Excess Weapon Pu Disposition in BN-600 Reactor Using BFS-2 Facility.

KEY WORDS: BFS-62-3A, TRIGEX code, MMKKENO code, CONSYST/ABBN system, ABBN-93 nuclear data set, experimental data, criticality, reactivity effects, calculation model.

---

*) JNC International Fellow (10/12/2001 - 9/12/2002)
Reactor Physics Research Group, System Engineering Technology Division, O-arai Engineering Center, JNC, Japan.

JNC TN9400 2002-037
2002年6月

IPPE標準解析システムによるBFS-62-3A炉心の実験解析結果
(研究報告書)

ミハイル　セミョノフ*

要　旨

本報告書には、ロシアの臨界実験施設BFS-2で実施されたBFS-62-3A炉心の実験解析結果を示す。本研究の目的は、ロシアの高速発電所BN-600のハイブリッド炉心に関する核特性解析コードTRIGEXの精度を検証することである。

実験体系の解析モデル及び解析結果と実験結果の比較を示した。解析には主として拡散計算コードTRIGEXコードを使用した。実験体系の非均質性を考慮するためにFFCPコードを使用してセル平均のマクロ及びミクロ断面積を作成し、TRIGEXコードで使用した。また、厳密な体系モデルにMMKKENOコードを適用したモンテカルロ計算結果も示した。モンテカルロ計算結果は、臨界性の基準解析値及び決定論で得られる各種補正値の検証に用いた。いずれの解析も、断面積データはABBN-93システムをベースとしCONSYSTコードで処理したものを使用した。

解析対象としたパラメータは、臨界性、制御棒価値(CRW)、ナトリウムボイド反応度効果(SVRE)、核分裂反応率分布及び中心反応率比（スペクトルインデックス）である。

TRIGEXコードによる解析結果と実験結果の差は、概ね下記の値以内であった。

臨界性；0.1%Δk/k、制御棒価値；6%

燃料領域の核分裂反応率分布；4%、SVRE；0.2pcm/kg・Na

なお、本研究は、ロシア余剰核兵器解体プルトニウム処分協力のために実施しているロシア物理エネルギー研究所(IPPE)のBFS-2臨界実験装置を利用したJNC-IPPE共同研究に関連して実施したものである。

キーワード：BFS-62-3A, TRIGEXコード、MMKKENOコード、CONSYST/ABBNシステム、ABBN-93核データセット、実験データ、臨界性、反応度効果、解析モデル

*：大洗工学センター　システム技術開発部　中性子工学グループ
国際特別研究員（2001年12月10日～2002年12月9日）

CONTENTS

Abstract in English i
Abstract in Japanese ii
Contents iii
List of tables iv
List of figures v
1. INTRODUCTION 1
2. EVALUATION OF BFS CRITICAL ASSEMBLY NEUTRONIC CHARACTERISTICS 2
2.1. General Approach and Method of Analysis 2
2.2. BFS-62. Brief Description of Critical Assembly 9
3. CALCULATION RESULTS 15
3.1. Criticality Evaluation 15
3.1.1. Results of Monte-Carlo Calculations 15
3.1.2. Results of TRIGEX Calculations 17
3.1.3. Results of TWODANT Calculations 19
3.2. Evaluation of Spectral Indices 21
3.3. Sodium Void Reactivity Effect (SVRE) 23
3.4. Control Rod Worth (CRW) 27
3.5. Reaction Rate Distribution 30
3.5.1. Radial Direction 30
3.5.2. Axial Direction 32
4. RELATIVE ANALYSIS OF CALCULATION AND EXPERIMENTAL RESULTS 35
4.1. Criticality and Spectral Indices 35
4.2. Sodium Void Reactivity Effect 37
4.3. Control Rod Worth 39
4.4. Reaction Rate Distribution 41
5. CONCLUSION 46
6. ACKNOWLEDGEMENTS 47
REFERENCES 48
APPENDIX: BFS-62-3A. Homogeneous Nuclear Densities A-1

LIST OF TABLES

Table 1. Parameters of BFS-62-3A assembly

Table 2. Monte-Carlo calculation results

Table 3. TRIGEX calculation results

Table 4. Results of transport correction factors by TWODANT code for BFS-62-3A

Table 5. Results of spectral indices on BFS-62-3A

Table 6. Comparison of SVRE obtained by two codes

Table 7. Results of SVRE calculation

Table 8. Results of CRW calculation (deterministic)

Table 9. Results of CRW calculation (Monte-Carlo method)

Table 10. Calculation results of the radial fission rate distributions

Table 11. Calculation results of the axial fission rate distributions

Table 12. Comparison of experimental and calculation criticality values

Table 13. Comparison of C/E values of the spectral indices

Table 14. Comparison of experimental and calculation SVRE values

Table 15. Comparison of C/E values of CRW

Table 16. Comparison of C/E values of radial fission rate distributions

Table 17. Comparison of C/E values of axial fission rate distributions

LIST OF FIGURES

Fig. 1. Calculation sequences using TRIGEX and MMKKENO codes

Fig. 2. BFS assembly structure

Fig. 3. Preparation of calculation model for FFCP

Fig. 4. BFS-62-3A assembly layout

Fig 5. Structure of fuel cells of BFS-62 assembly

Fig. 6. Rods of BFS-62

Fig. 7. BFS-62-3A. Two-dimensional R-Z models

Fig. 8. Location of the voided region

Fig. 9. Region-wise SVRE components

Fig. 10. Experiment control rod positions

Fig. 11. Efficiency of the control rod mock-ups

Fig. 12. Location of measurement points

Fig. 13. Central part of the modified 2D R-Z model

Fig. 14. SVRE. The Comparison of calculation and experimental results

Fig. 15. C/E values for control rod worth

Fig. 16. CRW calculated for "As-Built" model

Fig. 17. Fission rate distributions and C/E values in radial direction

Fig. 18. Fission rate distributions and C/E values in axial direction

1. INTRODUCTION

BFS-62 experiments are currently used as "benchmarks" for verification of IPPE and JNC codes and nuclear data, which have been used in the study of loading a significant amount of Pu in fast reactors.

This work is closely related to the JNC-IPPE Collaboration on "Experimental Investigation of Excess Weapon Pu Disposition in BN-600 Reactor Using BFS-2 Facility" on verification of neutronics analysis TRIGEX code /1/ and ABBN-93 cross-sections set /2/ used at the SSC RF IPPE and OKBM for design development and justification of the BN-600 reactor hybrid core.

The short description of the critical assembly BFS-62-3A – the third model of series of critical assemblies studying BN–600 reactor with hybrid MOX-zone and steel reflector - is given in this report. Calculation methods and codes that were used for calculation analysis of the experiments performed on this assembly are described in Chapter 2. The following parameters were analysed and discussed: criticality, traverses of fission rates, Sodium Void Reactivity Effect (SVRE), spectral indexes, efficiency of control rods mock-up. The analysis of the calculation accuracy on these parameters is the main goal of given work.

Calculation results on critical assembly BFS-62-3A are given in Chapter 3. Comparison with experimental data is described in Chapter 4. Deviations of calculation and measured results are summarized in Conclusion (Chapter 5).

2. EVALUATION OF BFS CRITICAL ASSEMBLY NEUTRONIC CHARACTERISTICS

2.1. General Approach and Method of Analysis

The main series of calculations were performed using TRIGEX code with ABBN-93 cross-section set, that had to be verified within JNC-IPPE Collaboration on "Experimental Investigation of Excess Weapon Pu Disposition in BN-600 Reactor Using BFS-2 Facility". In addition to these calculations, precise evaluations were also made by using MMKKENO /3/ and TWODANT /4/ codes. Calculation sequences using TRIGEX and MMKKENO codes are presented in Fig. 1. Below given are some details.

All calculations were made on the basis of the common system of group cross-section set: ABBN-93, using the ABBN93.01a version of working binary library.

It should be noted that all BFS assemblies are composed of 5.0 cm-diameter tubes spaced in hexagonal lattice with 5.1 cm pitch. In each tube, a column was composed of about 4.7 cm diameter pellets with different materials, which, as a rule, could be united into the standard cells. Geometrical structure of BFS assemblies is shown in Fig. 2.

In order to make calculations and prepare individual requests for analytical work, so-called "reference" (or "as-built") heterogeneous model was specified for assembly. In this model, specific composition was used for each type pellet to be put in the tubes. For some of them (for example, plutonium), clad (as a rule made of stainless steel) and core (plutonium) of the pellet were separated into different zones. This reference model served for preparation of homogeneous models, as a rule, by averaging compositions of some pellets with their volume weights, i.e. net material balance was maintained. Difference between results obtained in homogeneous and heterogeneous models is called "heterogeneous" correction. The concept of heterogeneous model is given below.

In 3D analysis, four calculation sequence options can be considered. Let us call these as "homogeneous" (#1) and "heterogeneous" (#2) calculations performed by TRIGEX code, «homogeneous» (#3) and «heterogeneous» (#4) calculations performed by Monte-Carlo high precision code: MMKKENO.

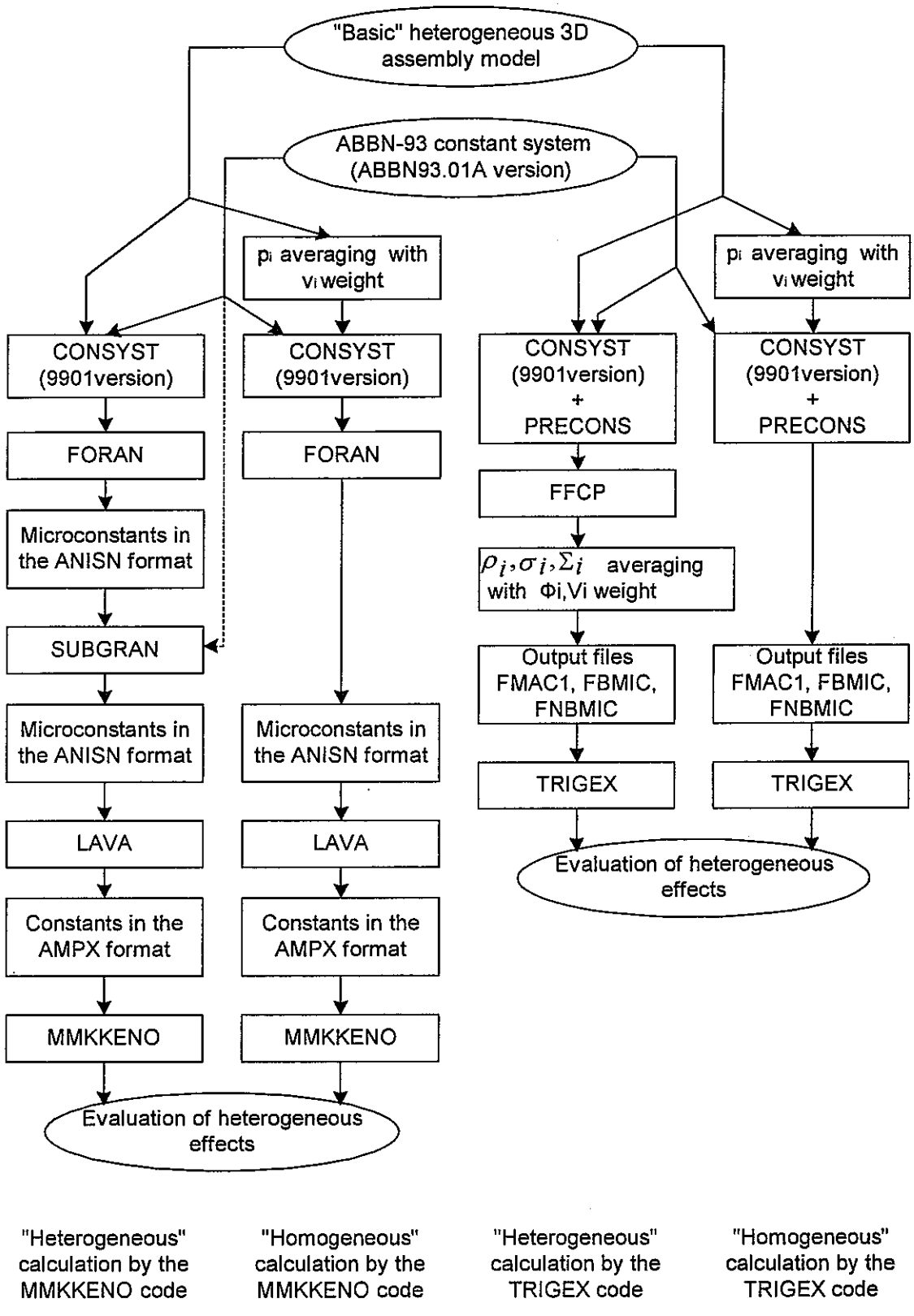

Fig. 1. Calculation sequences using TRIGEX and MMKKENO codes

Here ρ, V, Φ, σ and Σ – nuclear density, volume, neutron flux, micro and macro cross-sections, respectively.

#1. Calculation on the first sequence is based on 3D model of critical assembly with the real arrangement of all BFS tubes including control rod mock-up. In this model, tubes are filled with homogeneous compositions resulted from averaging material compositions of the pellets forming cells (of the core, axial reflectors, radial blanket, etc.), tube, in which pellets are placed, and, if necessary, inter-tube sticks. These sticks are used (although, not always) for decreasing the volume of hollow inter-tube space and making material composition of the model more adequate to that of the real reactor (in which there is no hollow space). Using CONSYST /5/ code 26 grouped self-shielded micro and macro constants are prepared for each homogeneous physical zone. If the radial steel reflector is used, total cross section for the core was self-shielded on the first harmonic, while the total cross section of the steel reflector was self-shielded on zero harmonic (i.e. by averaging with the neutron flux weight).

On the next stage, neutronic characteristics of the whole core are evaluated using TRIGEX code, and all necessary information is obtained. As a rule, the following parameters are used for fast core calculations:

- number of energy groups – 18 (including 17 groups corresponding to the standard ABBN groups from 1 to 17, and the last, 18^{th} group incorporating ABBN groups from 18 (below 100 eV) to 26);
- calculation mesh with one point per tube (5.1 cm spacing) and improved coarse mesh method;
- correction of b_j factors on the basis of preliminary 3D calculation.

#2. In heterogeneous calculation option based on the TRIGEX code, heterogeneous model of critical assembly is used. Using the same CONSYST code, constants are evaluated for all pellets describing the basic cells of the subassembly, and supplied to the input of the FFCP code /6/. This code evaluates distribution of group fluxes over the cell by the first flight collision probability (FFCP) method. Then averaging of multi-group macro constants is made within the cells with the weight of neutron fluxes and pellet volumes. Averaged (homogenized) macro constants are saved into the standard input files of TRIGEX code. Further calculation is made in the way similar to that of the first option. Thus, within the framework of TRIGEX code package, heterogeneity is taken into account by additional calculation made by FFCP code.

It is especially important that FFCP code is capable of making calculations of the cell in a subgroup approximation with taking into account one or more resonance nuclides (these are, as a rule, ^{235}U, ^{238}U, ^{239}Pu and Fe isotopes). For this purpose, FFCP code addresses directly ABBN-93 library and uses its section of subgroup parameters (26 groups). Operating in this mode, FFCP code calculates subgroup neutron fluxes and makes appropriate averaging of macro constants.

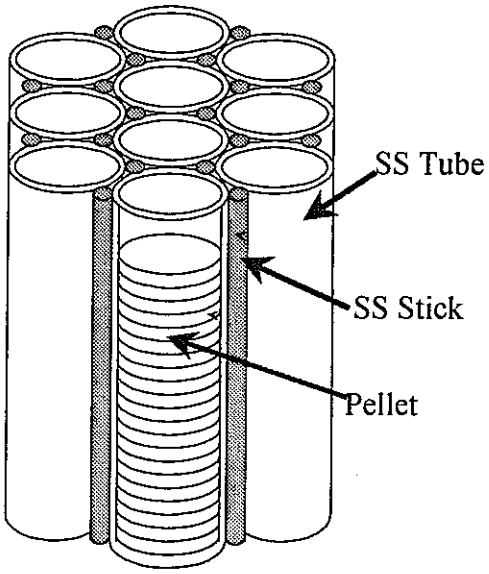

Fig. 2. BFS assembly structure

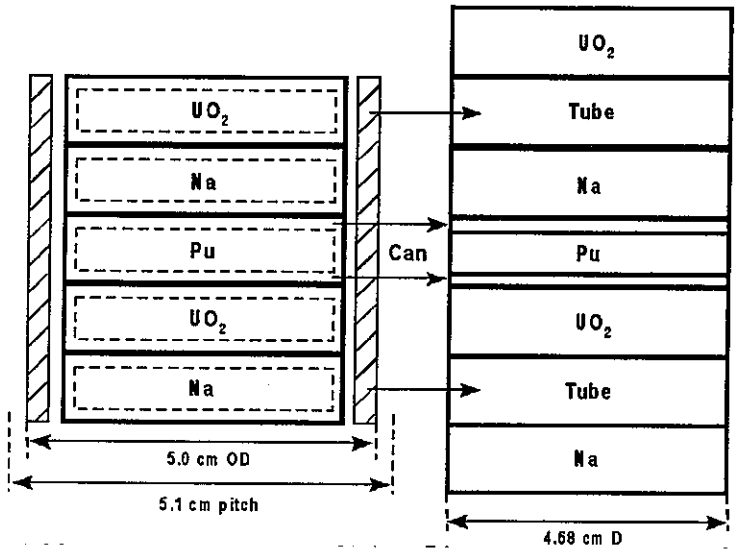

Fig. 3. Preparation of calculation model for FFCP

Calculation structure of FFCP code is a set of slab layers. This is very convenient for describing BFS cells: the layer of the original thickness simulates each pellet. There is one specific point, namely; BFS cylindrical tube containing pellets is taken into account by adding to the layers simulating pellets several new layers of thickness and composition corresponding to those of the tube and sticks. Sequence of preparation of geometrical calculation model of FFCP code is shown in Fig. 3 as an example.

#3. Geometrical model for homogeneous calculation using code MMKKENO is identical to similar model for TRIGEX code. Compositions of physical zones are also identical. Preparation of self-shielded macro constants is carried out by CONSYST code on the basis of ABBN-93 constants library. Formation of constants input file for MMKKENO code is made in two stages: on the first stage, constants are saved in

ANISN format /7/ using FORAN code /8/, and on the second stage they are converted into AMPX format /9/ using LAVA code from American code package: SCALE4.3 /10/.

Calculation by MMKKENO code is made by using Monte-Carlo method in multi-group (299 groups) approximation. Anisotropy of inelastic and elastic scattering is taken into account respectively in P_1- and P_5-approximations. Resonance self-shielding of the cross sections is evaluated on homogeneous compositions for infinite medium. Algorithm of preparation of the total cross section (on zero or the first harmonic) is completely coordinated with that for TRIGEX code, i.e. self-shielding for the steel reflector and the core are made by zero and first harmonics, respectively.

#4. In geometrical model of heterogeneous calculation using Monte-Carlo method by MMKKENO code, each single pellet and its can, BFS tubes and inter-tube sticks are modeled separately. Calculation model almost fully complies with the real structure of assembly without using any approximations. Like in all other cases, evaluation of self-shielded constants is made by using CONSYST code. These constants are formed in ANISN format.

Heterogeneous resonance cross-section blocking can be made in two ways. The first one is based on theorem of equivalence /11/ of resonance absorption in heterogeneous and homogeneous media. Practically, this means that correction depending on mean chord of BFS pellet is added to dilution cross section evaluated for infinite medium. The most simple expression of the correction is $1/\rho l$, where ρ - density of resonance absorber, and $l=4V/S$ – mean chord (V- pellet volume, S – surface area). Heterogeneous blocking in this case is taken into account by means of so-called δ-scattering material (D-SC). More details on the issue of taking into account heterogeneity for resonance self-shielding evaluation are given in /5/.

In high precision analysis, resonance blocking was taken into account by making calculations in the subgroup approximation. In this case, upon completion of multi-group constants preparation, special code SUBGRAN was used for preparing constants for subgroup calculation using section of subgroup parameters (299 groups) of ABBN-93 library. The same code makes reformation of group constants file in ANISN format in such a way that the subgroup calculation is converted into the group calculation, although with higher number of groups (not exceeding 1000). After that, constants are converted into AMPX format and calculation is made using MMKKENO code. This

method of taking into account resonance blocking was used for evaluation of k_{eff} and reactivity effects, which can be obtained as the difference between k_{eff} values in two calculations:

$$\rho = \frac{1}{k_{eff}} - \frac{1}{k_{eff'}} = \frac{\Delta k_{eff}}{k_{eff} k_{eff'}} \qquad (1),$$

where k_{eff} and k_{eff}' – eigenvalues respectively for the reference and perturbed systems.

The TWODANT code was used for evaluation of transport effects for all diffusion calculation results. In order to make TWODANT code calculations, 2D cylindrical model that is equivalent to the homogeneous model for TRIGEX code was designed on the basis of reference assembly model. This means that in these models, volumes and material compositions of physical zones are identical. Zone heights in TRIGEX and TWODANT codes are equal, and radius value of cylindrical zone in TWODANT code was chosen on the volume conservation condition.

The constants base is practically the same as that used for MMKKENO code: the same version of working binary library of ABBN constants base system is used, as well as the same code for blocked macro constants preparation, namely: CONSYST. The only difference is in that TWODANT code is coupled directly to the output file in ANISN format. TWODANT code calculations were performed using 28-group breakdown of energy scale adopted in ABBN-93, corresponding to the multi-group algorithm of constants preparation. Algorithm of preparation of the total cross section is the same as that described above for TRIGEX and MMKKENO codes.

In order to obtain final result, several calculations were made with TWODANT code. First, these are calculations simulating diffusion approximation and S_8– transport approximation using method of discrete ordinates. Second, these are calculations made for different space meshes. As a rule, two calculations were performed in diffusion approximation. In the second calculation, half as large size of the mesh was used as compared to that used in the first calculation. It is clear that such calculations were made for decreasing effect of mesh error on the final result (as a rule, it was k_{eff} value) obtained by the following extrapolation to the infinitely fine spacing of the mesh /12/:

$$k_{eff}(\infty) = \frac{4k_{eff}(\Delta/2) - k_{eff}(\Delta)}{3} \quad (2),$$

where Δ - mesh size (usually equal to 2 cm), $\Delta/2$ – half as large mesh size, i.e. 1 cm; k_{eff} (∞) – k_{eff} value extrapolated to the infinitely fine mesh size. Evaluation of transport effect is determined as the difference of extrapolated k_{eff} values obtained in diffusion and S_8 – transport approximation for sufficiently fine meshes.

Coming to the end of the general description, it should be noted that in the course of calculations, special attention was paid to the agreement of different calculation sequences. This makes it possible to evaluate some effects and uncertainties (heterogeneity and transport nature). It should be noted once more that all calculations were made on the basis of the same constant values using the same code for preparation of blocked neutron cross-sections CONSYST, as well as that all models were carefully agreed in terms of their material composition.

2.2. BFS-62-3A. Brief Description of Critical Assembly

Series of BFS-62 critical assemblies have been designed for studying the changes in BN-600 reactor neutronics from existing state to hybrid core. All these assemblies are used for modeling reactor state prior to refueling, i.e. with all control rod mock-ups withdrawn from the core.

The first assembly in this series (BFS-62-1) is an analogue of reactor in operation. There are three fuel regions in the core: Inner Core (IC), Middle Core (MC) and Outer Core (OC). Fuel is UO_2 with different enrichment. Both radial and axial blankets consist of depleted uranium dioxide.

BFS-62-2 assembly is different from BFS-62-1 by the radial blanket structure. In 62-2 assembly, 120° sector of radial reflector located outside the core is made of stainless steel, natural enrichment boron carbide being located behind this sector.

BFS-62-3A assembly is a full-scale model of the BN-600 reactor hybrid core. Zone with MOX fuel was added like ring between MC and OC. Radial blanket is similar to that of BFS-62-2 assembly.

Characteristics of fuel rods of BFS-62-3A core and their number are presented in Table 1. Figures 4 and 5 present layout of the assembly, structure of the fuel cells and their heights. Figure 6 shows axial structure of each type of rod.

Assembly is made in the steel tubes located in hexagonal mesh with 5.1 cm pitch. Fuel and structural material pellets are placed in the tubes. Six Control Rods (CR) and six Safety Rods (SR) mock-ups are located in low enrichment zone (IC), and the rest twelve CR mock-ups are placed on the border of IC and MC as are shown in Fig. 4. Four BFS tubes simulate each control rod mock-ups.

Table 1. Parameters of BFS-62-3A assembly

Parameters	IC	MC	MOX	OC
Fuel	UO_2	UO_2	MOX	UO_2
Enrichment, at. %	15	18	17	21
Number of tubes:	595*)	222	336	237

*) Besides, there are 54 tubes not containing fissile material in IC.

It should be mentioned that there are two types of Na pellets at BFS facility – the old one "green" with some amount of hydrogen in NaOH and the new pellets "laser" without it. Region formed by new sodium pellets is similar key-hole ("key region") and marked with more deep colours at Fig. 4. The main parameters including radial fission rate distributions, SVRE and other were measured in this "key region".

All sizes shown on Figs. 5 and 6 are given for "green" sodium pellets.

Fuel cells have "mirror symmetry" relatively core midplane.

Experiments aimed at determining criticality, sodium void reactivity effect, control rod mock-up worth, reaction rate distribution and average fission cross section ratios were chosen for this report.

Experimental program has been arranged in such a way that effect of the steel reflector on the main characteristics of reactor model can be studied.

It should be mentioned that from this Chapter and further "core" means fuel regions with CR followers inside inner part, and "assembly" means assembly at whole (including blankets, reflector and shield).

List of abbreviations for figures 6:

LAB – Lower Axial Blanket

UAB – Upper Axial Blanket

UAS – Upper Axial Shield

Cu – Copper pellet

More detail description of the BFS-62-3A assembly see in references /13, 14/.

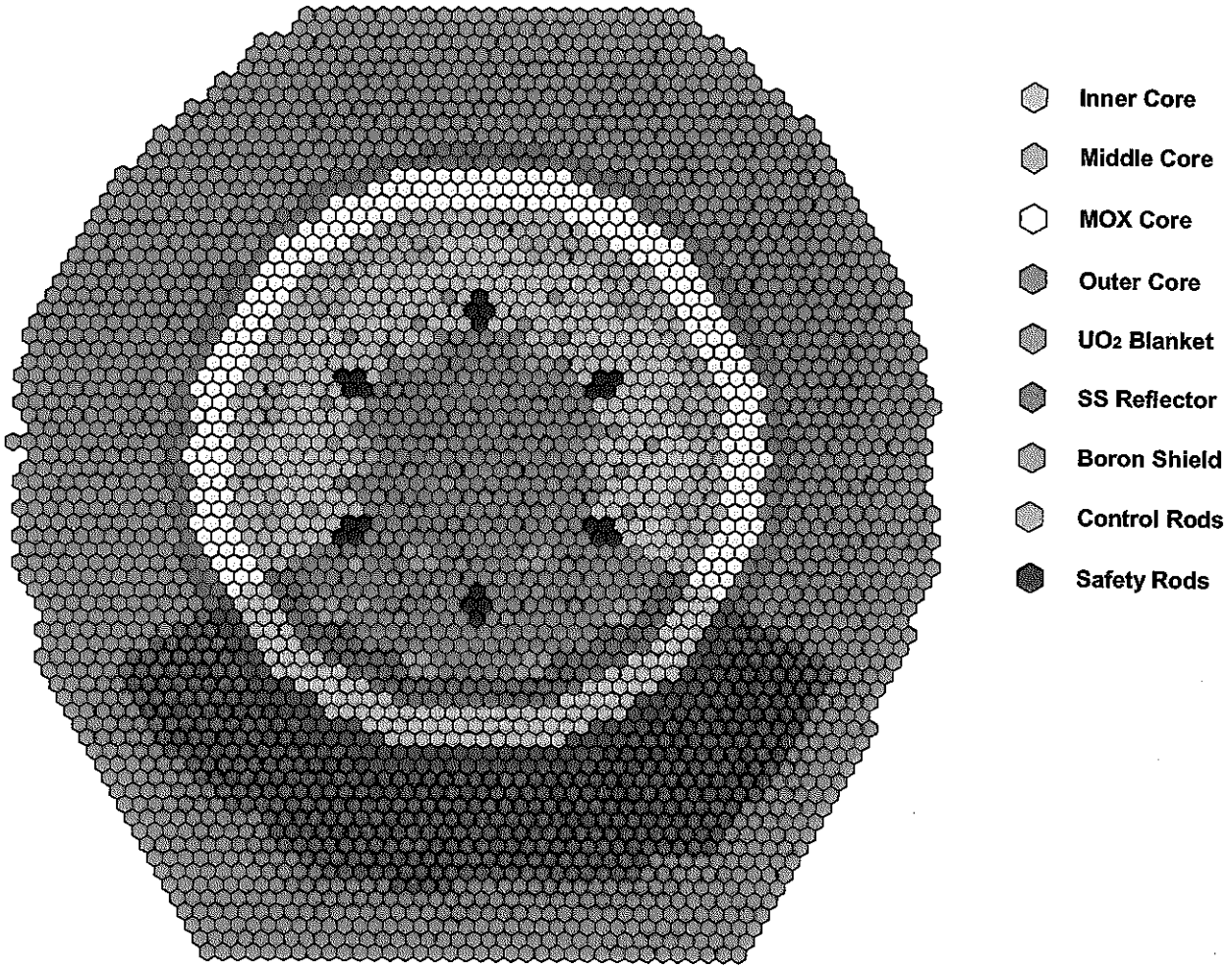

Fig. 4. BFS-62-3A assembly layout

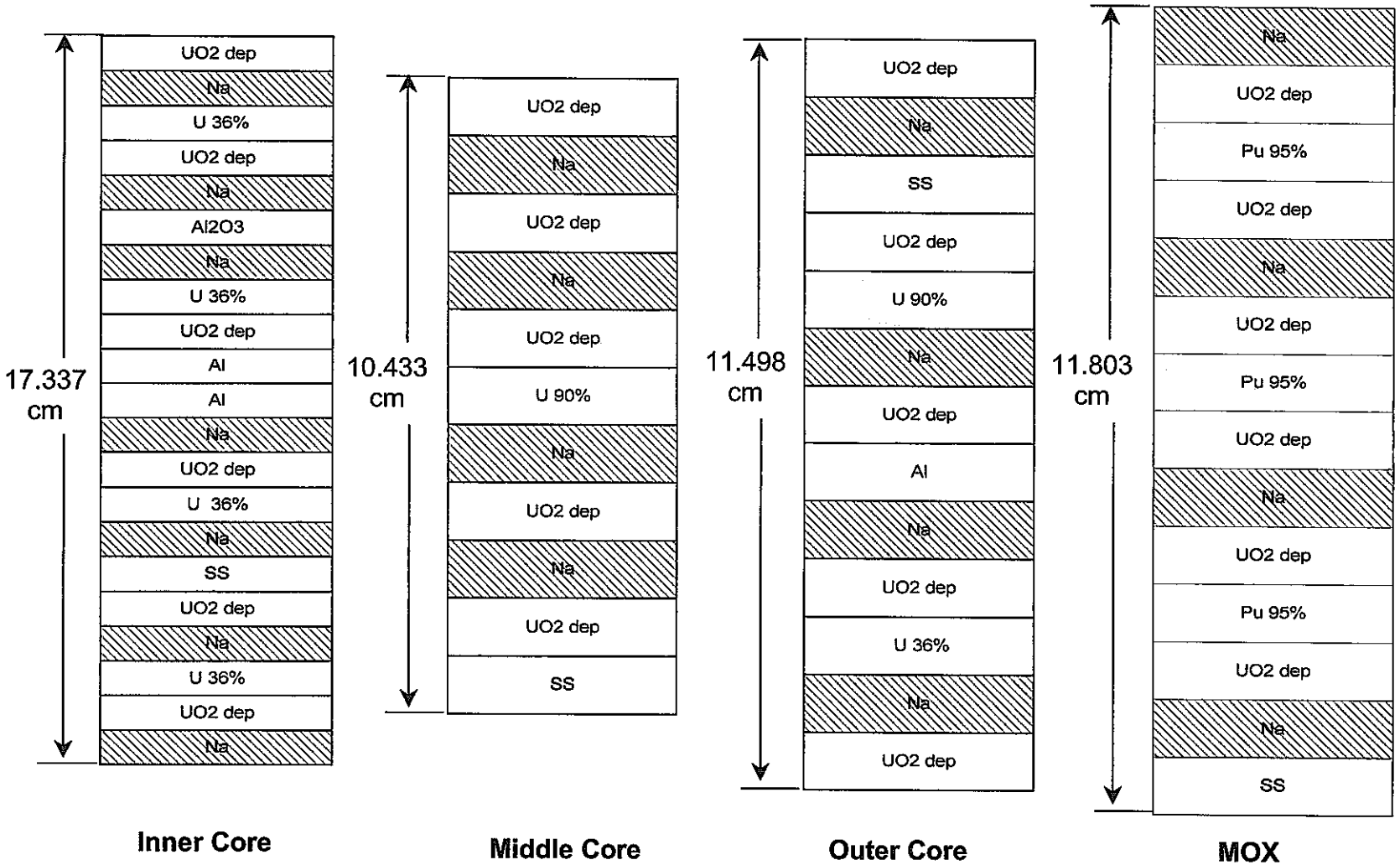

Fig 5. Structure of fuel cells of BFS-62 assembly

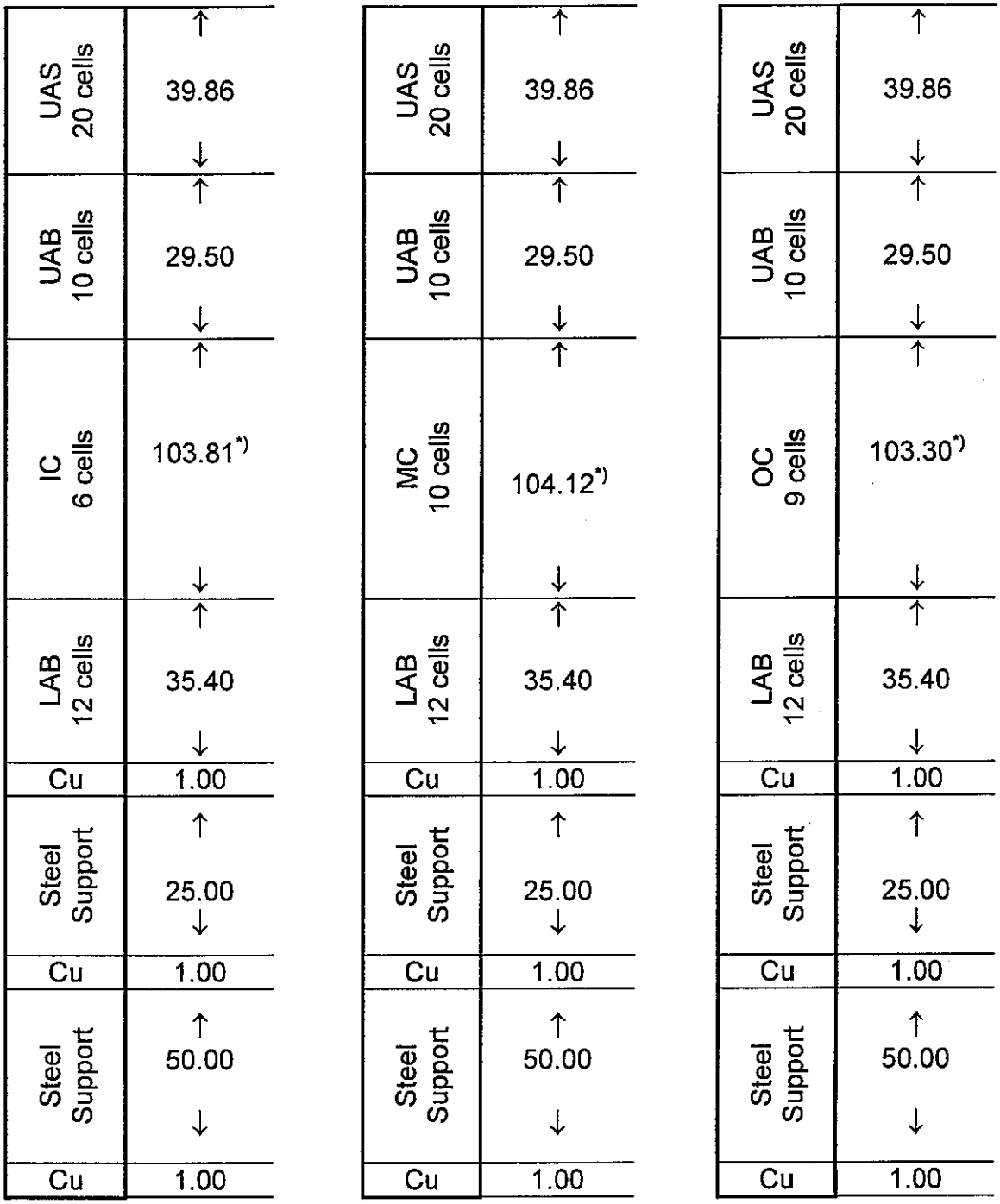

*) Average measured values

Fig. 6. Rods of BFS-62 (all sizes are given in cm)

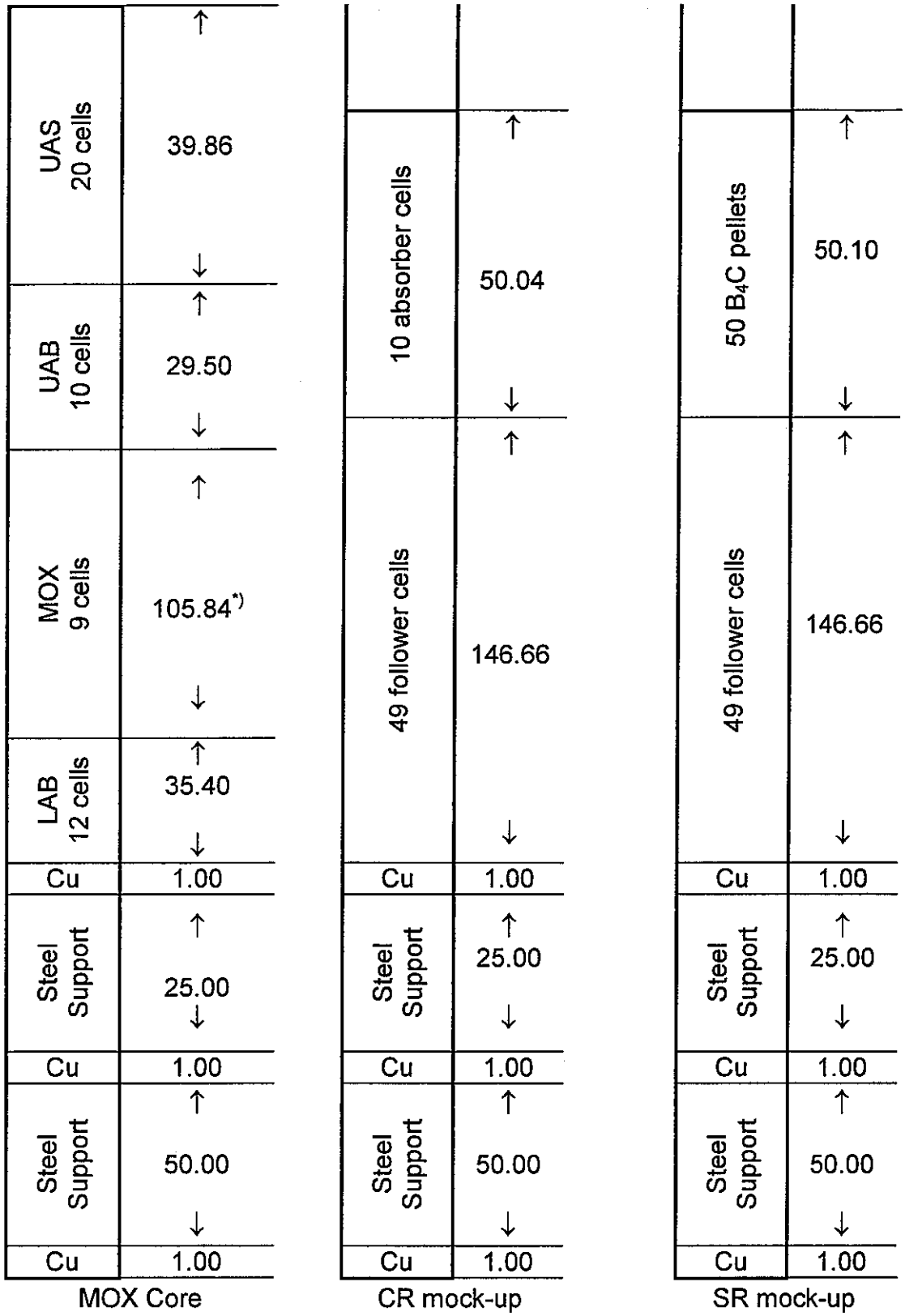

Fig. 6. Rods of BFS-62 (continued)

3. CALCULATION RESULTS

3.1. Criticality Evaluation

3.1.1. Results of Monte-Carlo Calculations

First of all, as was written above, so-called "reference" (or "as-built") heterogeneous model was specified for assembly. It means that calculation model includes practically all details of BFS-62-3A:

- Full layout is like on Fig. 4 (plus 3~6 rows of empty tubes on periphery);
- Total tube height and grid plate are under consideration;
- All pellets have the real sizes and weights;
- All canned pellets have cans with 0.03 cm in thickness except the Pu pellets, having 0.04 cm-thick can;
- All fuel rods have 2 sticks per tube.

It should be noted that additional experimental nuances (not marked on Fig. 4) were taken into account under constructing of this model in accordance with preprint /13/.

This reference model served the base for preparation of another heterogeneous and homogeneous models by averaging compositions of some pellets with their volume weights, i.e. net material balance was maintained. These models are:

1) Simplified heterogeneous model;

2) Exact homogeneous model;

3) Simplified homogeneous model.

Simplified heterogeneous model was constructed to determine "additional heterogeneity" effect, i.e. the difference between real heterogeneity effect and one calculated by FFCP. Remind that the FFCP code uses 1-D plate cell model with periodical boundary conditions. All pellets have the same radius (2.34 cm) and tube with sticks is presented like additional layers. Only fuel cells have heterogeneous description and only plutonium pellets have cans.

The homogeneous models were prepared to estimate total heterogeneous effect (exact homogeneous model), model and group collapsing effects (simplified homogeneous model).

Exact homogeneous model repeats "as-built" one in geometry but homogeneous nuclear densities are used instead heterogeneous.

Simplified homogeneous model was constructed with following approximations:

1) All axial sizes of the fuel tubes are adjusted:

- Bottom Blanket - 35.4 cm;
- Core height - 103.81 cm (experimental value for Inner Core);
- Upper Blanket - 29.39 cm (the thickness with "laser" Na);
- Axial Shield - 39.86 cm;

2) Axial sizes of the Control Rods are the same (like in the "pure core");

3) Layout is the same like for exact model except polyethylene tubes in Reflector (are changed by boron and stainless steal tubes);

4) Bottom part of the Support, Grid Plate and Upper (empty) part of the tubes are removed.

On next steps this model was adopted for creating TRIGEX model (3-D Hex-Z geometry) and TWODANT one (2-D R-Z geometry).

Calculations were performed with 299-group cross-section set. Moreover subgroup approximation was taken into account for U-238 isotope. Thus the total number of groups is equal 447. D-scattering method was applied for U-235 and Pu-239 isotopes (see Chapter 2.1). All calculation results have 10 millions active histories and statistical errors are in 0.015~0.017% range. Monte-Carlo results on criticality are summarized in Table 2.

Table 2. Monte-Carlo calculation results

	k-eff	Comments
Base Result	1.00163±0.00017	"As-built" Model, 299 gr. + subgroups
Estimated effects		
Heterogeneity Effect	+0.01315±0.00023	Ex. Hom. Mod.* → "As-built" Model
Model Effect	-0.00135±0.00021	Sim. Hom. Mod.** → Exact Hom. Mod.
Additional Heterogeneity	+0.00212±0.00024	Sim. Het. Mod.*** → "As-built" Model
Group Collapsing Effect	-0.00054±0.00021	28 groups → 299 groups

* Exact Homogeneous Model ** Simplified Homogeneous Model *** Simplified Heterogeneous Model

3.1.2. Results of TRIGEX Calculations

In the calculation model of each state, there is a description of the whole assembly including empty tubes on periphery. There are 59 calculation layers over the height of the model (all sizes are given in cm):

Support	-	2., 3., 5*4. (five regions, each with a thickness of 4 cm);
Lower Axial Blanket-		8*4.425;
Core	-	2*3.322, 4*4.344, 13*4.29, 4*4.344, 2*3.322;
Upper Axial Blanket-		2*3.1845, 3.021, 5*4.;
Axial Shield	-	3.689, 4*4., 3.697, 3.303, 3.087, 4.084, 4., 2.

First of all, thickness of geometrical layers is chosen in this way that the axial size was approximately equal to the lattice pitch in X-Y plane for improvement of algorithm convergence. To decrease mesh-size correction factor, these values can be slightly smaller. Then axial layers thickness is adopted to calculate all measured items including CRW with the same model. In the plane (X-Y), mesh size is equal to 5.1 cm. Nuclear densities for all calculation regions are listed in Appendix.

Cross-sections were prepared for the core using the FFCP code (resonance isotopes: uranium-238, uranium-235 and plutonium-239), and homogeneous approximation was used for the other zones. Since there are voids (areas that are not filled with the core composition) in the hexagonal cross section of BFS cell, additional layers containing tube and sticks composition are introduced on the uniform basis to the real cell description for making calculation by FFCP. This is made on condition of conservation of both thickness and nuclear densities of the pellets. The numbers and sizes of such layers were as follows:

- in IC cell: six 0.89018 cm thick layers;
- in MC cell: four 0.803719 cm thick layers;
- in MOX cell: five 0.727764 cm thick layers;
- in OC cell: five 0.708888 cm thick layers.

Criticality was determined for the initial state. Besides, heterogeneous and mesh-size effects were estimated by additional calculations.

Mesh-size correction factor f_c consists of two components – axial $f_c(z)$ and radial $f_c(r)$. It should be mentioned that standard TRIGEX calculations are performed on the

base of the improved coarse-mesh discretization technique of the diffusion problem which allows to decrease (but not reduce to zero) inaccuracy connected with coarse mesh pitch in (X-Y) plane. Such calculations are named ones with correction on coarse mesh pitch in (X-Y) plane. At the same time there is a possibility to use ordinary finite-difference method with one point per hexagon (calculation without correction). Group calculations are performed by using TRIGEX with correction on coarse mesh pitch in (X-Y) plane and without one for estimation of the radial component of this factor. The total number of axial layers is the same like under standard calculation.

Let's K_{eff}(C) means K_{eff} value obtained under standard calculation with correction, and K_{eff}(WC) – without one. In that case radial component can be written like:

$$f_c(r) = 1 + \alpha_r \frac{K_{eff}(C) - K_{eff}(WC)}{K_{eff}(C)} \quad (3),$$

and parameter α_r is equal to 0.25 /15/.

For estimation of the axial component additional group calculations are performed by using TRIGEX with correction on coarse mesh pitch in (X-Y) plane and with doubled number of calculation layers. Let's K_{eff}(h) means K_{eff} value obtained under standard calculation with usual thickness (h) of the calculation layers, and K_{eff}(h/2) – with doubled number of ones, i.e. twice as small thickness of layers (h/2). Then axial component can be written like:

$$f_c(z) = 1 + \alpha_z \frac{K_{eff}(h/2) - K_{eff}(h)}{K_{eff}(h/2)} \quad (4),$$

and parameter α_z is equal to 0.33 /15/.

Summarized TRIGEX results are presented in Table 3.

Table 3. TRIGEX calculation results

	k-eff	Comments
Homogeneous	0.98689	CONSYST+TRIGEX
Estimated effects		
Heterogeneity Effect	+0.0109	CONSYST+FFCP+TRIGEX
Mesh Effect	-0.0005	X-Y and Z Correction

3.1.3. Results of TWODANT Calculations

TWODANT code was used for evaluation of transport effect. Calculations were carried out using R-Z model with homogeneously prepared constants in 28-group approximation for initial state of the assembly. Since BFS-62-3A hasn't radial symmetry, the own models were constructed both for "key region" and for "green region".

The former model includes only "laser" sodium pellets and stainless steel reflector with natural enrichment boron carbide. The latter "green" model contains "laser" sodium in central part and "green" one into all the other regions. Also uranium blanket is installed on periphery. Models describing BFS-62-3A assembly are presented in Fig. 7.

Calculations were made in both diffusion and S_8-transport approximations. Calculation meshes with ~2 cm and ~1 cm pitch were used. Evaluation of transport effect is determined as the difference of extrapolated k_{eff} values obtained in diffusion and S_8 – transport approximation for sufficiently fine meshes. Average transport correction for BFS-62-3A was obtained like:

$$\langle f_{TR} \rangle = \frac{1}{3} f_{TR}(Laser) + \frac{2}{3} f_{TR}(Green) \qquad (5)$$

Results of transport correction factor evaluation are presented in Table 4.

Table 4. Results of transport correction factors by TWODANT code for BFS-62-3A

Model	Diffusion calculation	S_8-transport calculation	Transport correction
Key Region	0.98056	0.98566	0.0051
Green Region	0.98700	0.99091	0.0039
Average			0.0043

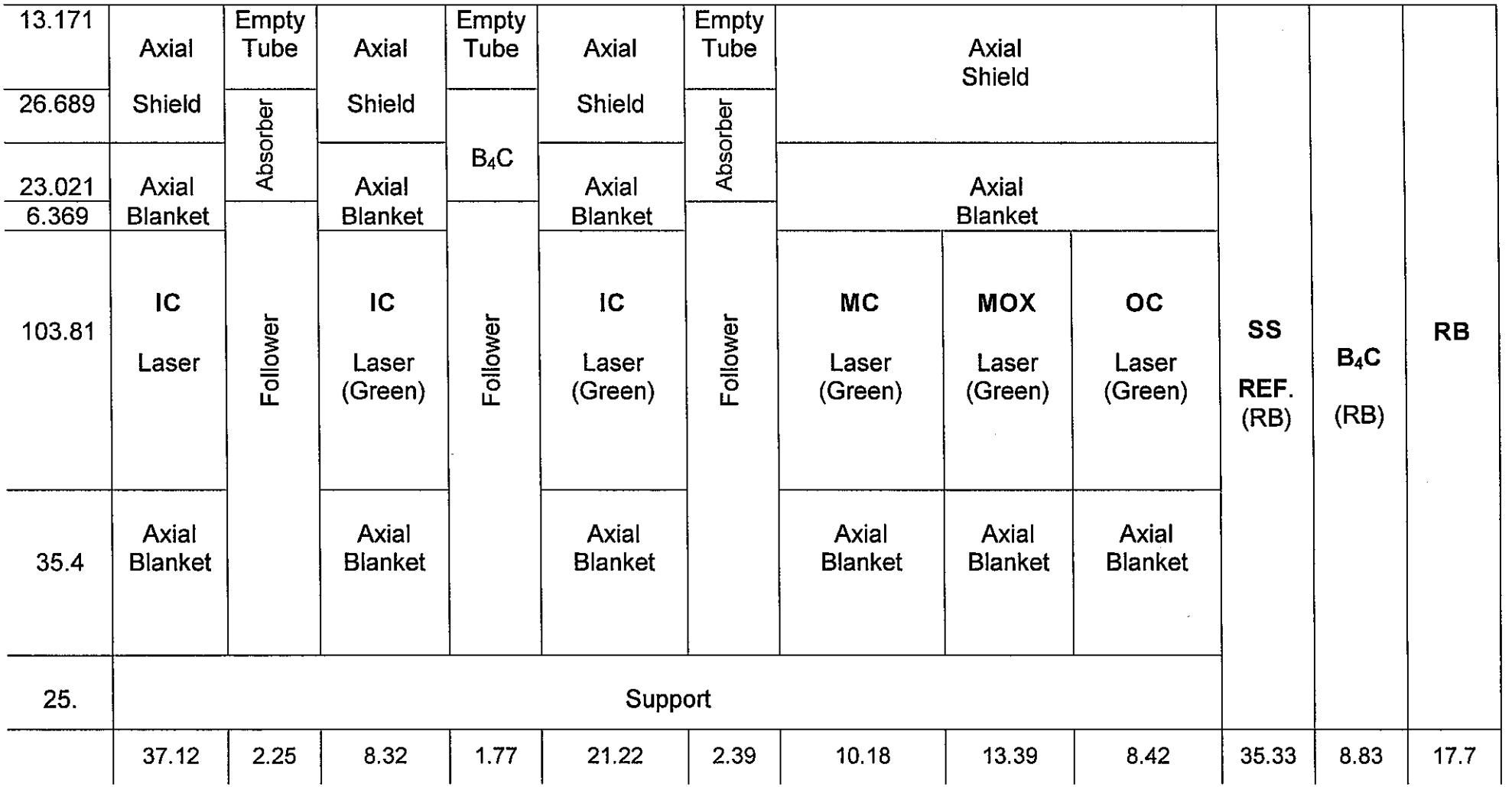

Fig. 7. BFS-62-3A. Two-dimensional R-Z models (all sizes are given in cm)
a) Laser direction
b) Green direction

3.2. Evaluation of Spectral Indices

This section presents the results of evaluation of fission cross sections ratios of the main fuel nuclides measured in the central area of the core. Experimental results on fission cross-section ratios were obtained by the small size fission chambers using calibration method in the thermal column. Chambers of 7 mm diameter are located in the inter-tube space. In the course of tests, these chambers are moved by means of manipulator vertically at 10 mm steps along the central cell axis. Thus, as a result of measurements, some value of the functional averaged over the cell is determined. Measurements in the core and calibration carried out in thermal (graphite) column are repeated. This cycle is repeated 5 to 10 times.

Below described is procedure of analytical reproduction of experimental results. First, "heterogeneous" calculation was made by TRIGEX code, i.e. calculation with constants prepared via FFCP code. However, it should be taken into account that "heterogeneous" constants are calculated for TRIGEX code in FFCP code by averaging with the weight of $V_j*\rho_{ij}*\varphi_j$ product, where i – index of isotope, j – index of BFS pellet included into the cell:

$$\langle \sigma_i \rangle = \frac{\sum_{j=1}^{M} \overline{\sigma}_{i,j} \bullet \rho_{i,j} \bullet \varphi_j \bullet V_j}{\langle \rho_i \rangle \bullet \sum_{j=1}^{M} \varphi_j \bullet V_j} \qquad (6) \qquad \text{where} \qquad \langle \rho_i \rangle = \frac{\sum_{j=1}^{M} \rho_{i,j} \bullet V_j}{\sum_{j=1}^{M} V_j}$$

ρ, V and φ – atom density, volume and neutron flux, respectively. This assures preservation of the general balance of reaction rates in the cell. The following parameter is measured in the course of tests:

$$\sim N_i \langle \varphi_j \bullet \sigma_i \rangle = N_i \frac{\sum_{j=1}^{M} \overline{\sigma}_{i,j} \bullet \varphi_j \bullet V_j}{\sum_{j=1}^{M} V_j} \qquad (7)$$

where N_i – number of atoms in the foil or fission chamber layer ("<>" sign means «average value»). So, averaging of cross sections (reaction rates) over the cell is required without taking into account concentrations of this isotope in the pellets:

$$\langle \sigma_i \rangle = \frac{\sum_{j=1}^{M} \overline{\sigma}_{i,j} \bullet \varphi_j \bullet V_j}{\sum_{j=1}^{M} \varphi_j V_j} \qquad (8)$$

As a rule, average values obtained using (6) relationship, do not differ much from the cross section values averaged by (8) relationship. Such correction taking into account the difference in the cross section values prepared in the course of cell evaluation with and without concentration weight was obtained by FFCP code. This correction (f_{het}) was introduced to the result obtained by TRIGEX code.

Also transport corrections (f_{tr}) were calculated. These factors are negligible and not larger than 0.5%.

Results of analysis are presented in Table 5, where:

F238 / F235 means fission of uranium-238 divided on fission of uranium-235, etc.

Table 5. Results of spectral indices on BFS-62-3A

Index	TRIGEX	f_{het}	f_{tr}	C (Corr)*
F238/F235	0.02242	0.9263	0.995	0.0207
F239/F235	0.9645	0.9699	0.999	0.9345

* Corrected calculation result

3.3. Sodium Void Reactivity Effect (SVRE)

In this assembly, sodium pellets were replaced with the empty boxes in 60° sector for all zones (see Fig. 8): IC, MC MOX and OC. The voiding area covered the core and the upper axiaPl blanket. It should be noted that sodium was not removed from the control rod mock-ups and from the standard control rods of the assembly (marked by ⊗). Thus, in the course of tests, 118 IC FR, 37 MC FR, 58 MOX FR and 46 OC FR were reassembled.

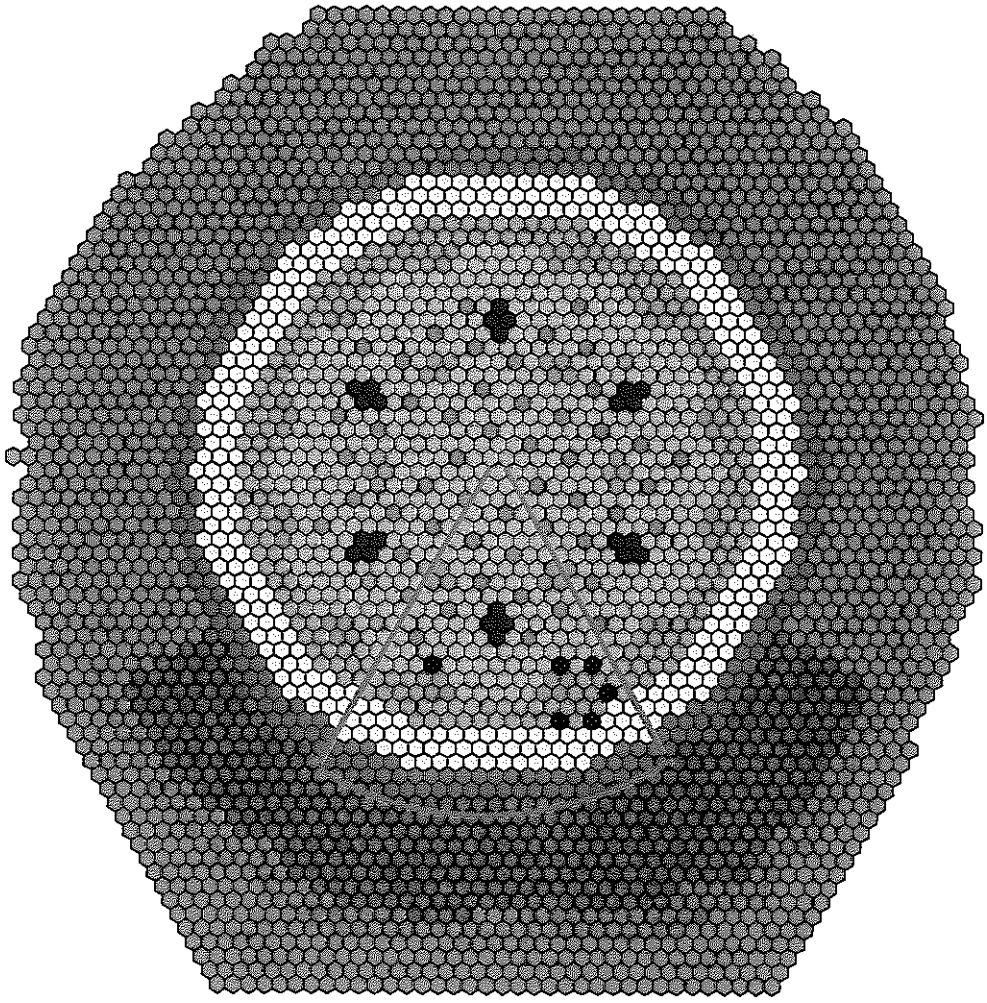

Fig. 8. Location of the voided region

This reactivity effect was calculated using the TRIGEX code package as a difference between the results of two direct heterogeneous calculations (with/without sodium) like:

$$RE_i = \frac{K_{eff}^0 - K_{eff}^i}{K_{eff}^0 \times K_{eff}^i}.$$

Here index ***i*** means perturbed state and index ***0*** is related to initial state of the assembly. Considering of small values of the measured effects (about 10 ¢) the convergence criteria were increased: $1*10^{-5}$ for local fission sources and $5*10^{-6}$ for k_{eff}. Calculations were performed step by step, i.e. under successive sodium removal from region to region.

Then the mesh-size and transport corrections were applied to obtain final results; the difference is that these corrections are calculated not for K_{eff} value but for reactivity effects (RE) directly. It means that RE values are used in formulas, mentioned above (Chapter 3.1.2), instead K_{eff} values.

Mesh-size correction factor $\mathbf{f_c}$ for reactivity effect consists of two components also – axial $\mathbf{f_c(z)}$ and radial $\mathbf{f_c(r)}$. Let's ***RE***(C) means reactivity effect value obtained under standard calculation with correction on coarse mesh in (X-Y) plane, and ***RE***(WC) – without one. In that case radial component can be written like:

$$f_c(r) = 1 + \alpha_r \frac{RE(C) - RE(WC)}{RE(C)} \qquad (9)$$

and parameter α_r is equal to 0.4 /15/.

Let's ***RE***(h) means reactivity effect value obtained under standard calculation with usual thickness (h) of the calculation layers, and ***RE***(h/2) – with doubled number of ones, i.e. twice as small thickness of layers (h/2). Then axial component can be written like:

$$f_c(z) = 1 + \alpha_z \frac{RE(h/2) - RE(h)}{RE(h)} \qquad (10)$$

and parameter α_z is equal to 1 /15/.

Transport corrections were evaluated on the base 2-D R-Z "key region" model in 28-group approximation. Calculations were made in both diffusion and S_8-transport approximations. Calculation meshes with ~2 cm and ~1 cm pitch were used also. But first of all it should be satisfied that R-Z model describes this effect good enough. For this purpose two series of diffusion homogeneous calculations were done by using TWODANT for 2-D geometry and by using TRIGEX for 3-D Hex-Z geometry. The

TWODANT results were divided by six. The comparison of two types of the calculations is presented in Table 6.

Table 6. Comparison of SVRE obtained by two codes (pcm, 10^{-5} $\Delta k/kk'$)

Voided Region	TRIGEX	TWODANT	TRIGEX-TWODANT
Inner Core	-29.0	-28.8	-0.2
Middle Core	-10.7	-11.2	+0.5
MOX Core	-26.1	-27.7	+1.6
Outer Core	-48.8	-48.3	-0.5

A good agreement between two types of results is observed and discrepancies are about 1 pcm. So, there is possibility to use R-Z model for estimation of transport correction. TRIGEX calculation results and corrections are presented in Table 7.

Table 7. Results of SVRE calculation, (pcm)

Voided Region	TRIGEX	Mesh	Transport
Inner Core	-66.5	-1.93	+3.15
Middle Core	-15.8	-0.30	+1.12
MOX Core	-44.4	-0.66	+6.20
Outer Core	-63.3	-0.71	+1.61

To understand the nature of SVRE changes from region to region, the studying of SVRE behavior with taken into account "First Order Perturbation Theory" was made by using the TRIGEX code. These investigations have shown that the leakage component of SVRE is increased droningly from core center to periphery, in which connection the defining value has axial leakage at first but the radial one predominates on the last steps. The non-leakage component has maximum in the middle part of the core.

The most intensive region is the middle core – in this region leakage component is the least and non-leakage one is the largest and the values of these components are very close. Region-wise SVRE and its components are presented on Fig. 9. So the sodium quantity is differed visibly from region to region (from 730 g to 640 g per tube),

more suitable to compare these effects not in absolute values but normalized on 1 kg of removed sodium.

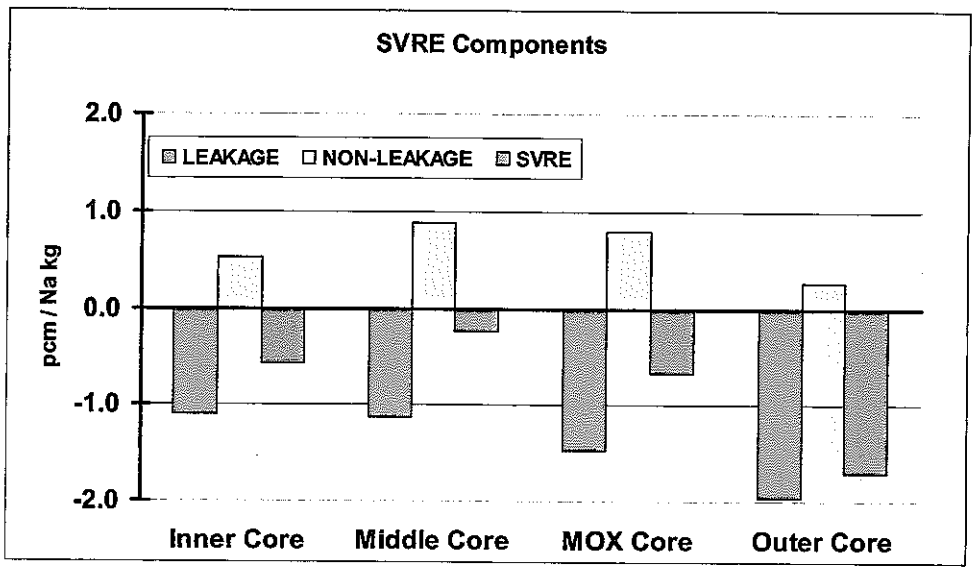

Fig. 9. Region-wise SVRE components

3.4. Control Rod Worth (CRW)

The program of measurements of CRW was based on that the worth of two diametrically opposite mock-ups from each CR and SR ring (see Fig. 10) are measured by re-assembly method.

Initial composition of CR mock-up (Fig. 6) was changed as follows. In the lower section, 20 cells were kept to simulate control rod follower, then 16 cells of absorber section were placed, and after that 20 more cells of control rod follower were introduced. The composition of modified SR mock-up was similar to this: 20 control rod follower cells were put at the top and at the bottom, with 73 boron carbide pellets in between.

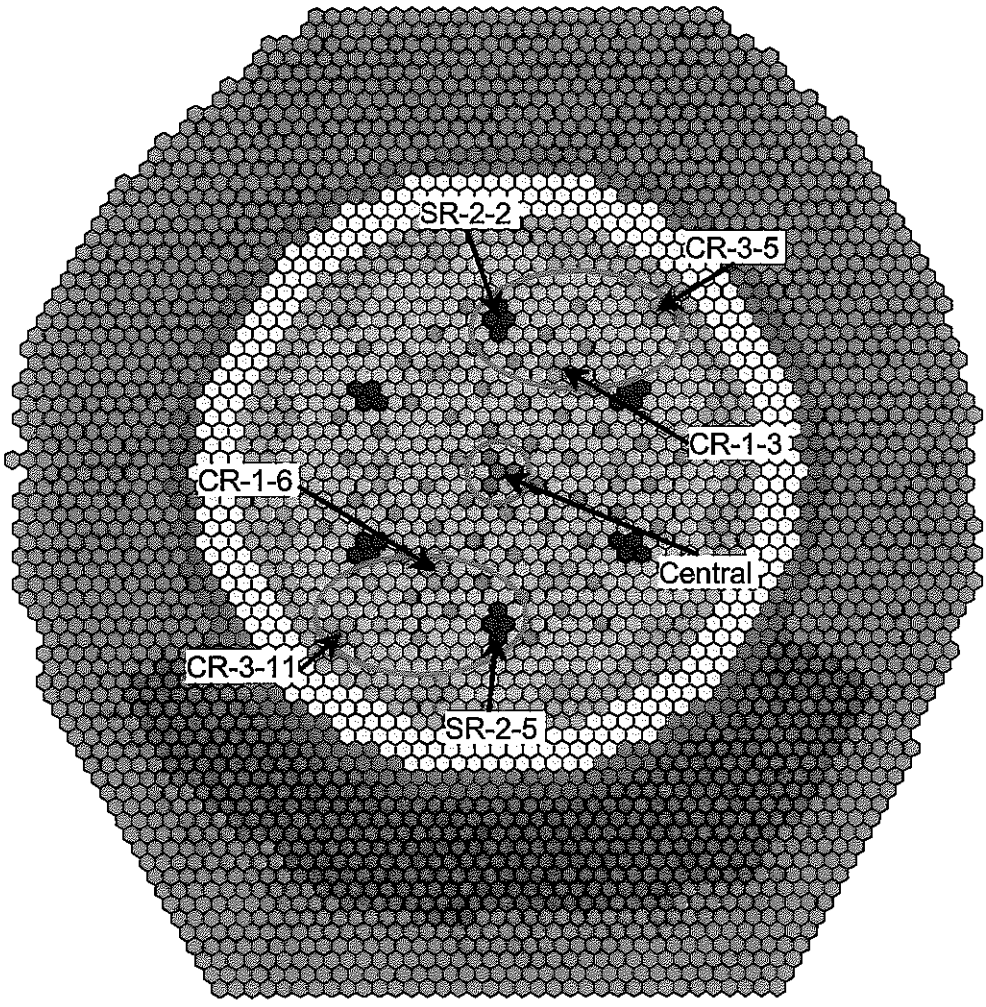

Fig. 10. Experiment control rod positions

Worth measurement procedure consisted of two stages. On the first stage, reactivity of the control rod follower and then that of B_4C was measured with respect to the empty channel. The net effect was determined as a sum of two reactivity values. Experimental error of such measurements is approximately 1.5% and basic components of the error are uncertainty of six-group delayed neutron parameters, inaccuracies of mathematical models, statistical uncertainties and so on /14/.

Calculation value of reactivity effect was determined as a difference between the results of two direct homogeneous diffusion evaluations: one for the initial state and the other – for absorber inserted into the core. Then the heterogeneous, mesh-size and transport corrections were applied to the obtained results. The procedure of definition of the correction factors was the same like for SVRE. It should be mentioned that two R-Z models were used by TWODANT code. "Laser" model was used for CR-1-6, CR-3-11 and for SR-2-5, but while "Green" model was used for CR-1-3, CR-3-5 and for SR-2-2. Both models are used for definition of the transport correction for central CR worth. Averaged factor in this case is

$$\langle f_{TR} \rangle = \frac{1}{3} f_{TR}(Laser) + \frac{2}{3} f_{TR}(Green) \tag{11}$$

Results of the control rod mock-up worth and correction factor values are presented in Table 8.

Table 8. Results of CRW calculation (deterministic)

Type	Ring	Position	TRIGEX (pcm)	Heter. (%)	Mesh (%)	Transport (%)	Total (%)
CR		Center	348.2	-1.5	+2.1	-5.6	-5.3
CR	1	3	352.1	-0.2	+2.3	-4.7	-2.6
CR	1	6	341.2	-3.1	+2.4	-5.6	-6.3
SR	2	2	586.5	-2.9	+4.0	-5.5	-4.4
SR	2	5	578.2	-4.4	+3.6	-6.2	-7.0
CR	3	5	313.7	-0.2	+2.2	-2.6	-0.6
CR	3	11	289.8	-3.7	+2.0	-2.5	-4.2

The calculations for more precise determination of the control rod worth were done using the Monte-Carlo method by MMKKENO in homogeneous approximation. The same models like TRIGEX were used. The calculations were performed with 299-

group energy structure and P_5-approximation of the elastic scattering. All calculations were done with 50 millions of active neutron histories. Thus, it was proposed that total correction (diffusion, mesh-size and group), except heterogeneous, will be defined more precisely, however relative statistical error was found about 4%. Results of these calculations are presented in Table 9.

Table 9. Results of CRW calculation (Monte-Carlo method)

Type	Ring	Position	Region	MMKKENO (pcm)
CR		Center	Laser	349±10 *)
CR	1	3	Laser	325±10
CR	1	6	Laser	322±10
SR	2	2	Green	537±10
SR	2	5	Laser	556±10
CR	3	5	Green	284±10
CR	3	11	Laser	287±10

*) Statistical error

All calculation data and experimental results are shown on Figure 11. Positive direction points to stainless steel reflector and negative – to uranium blanket.

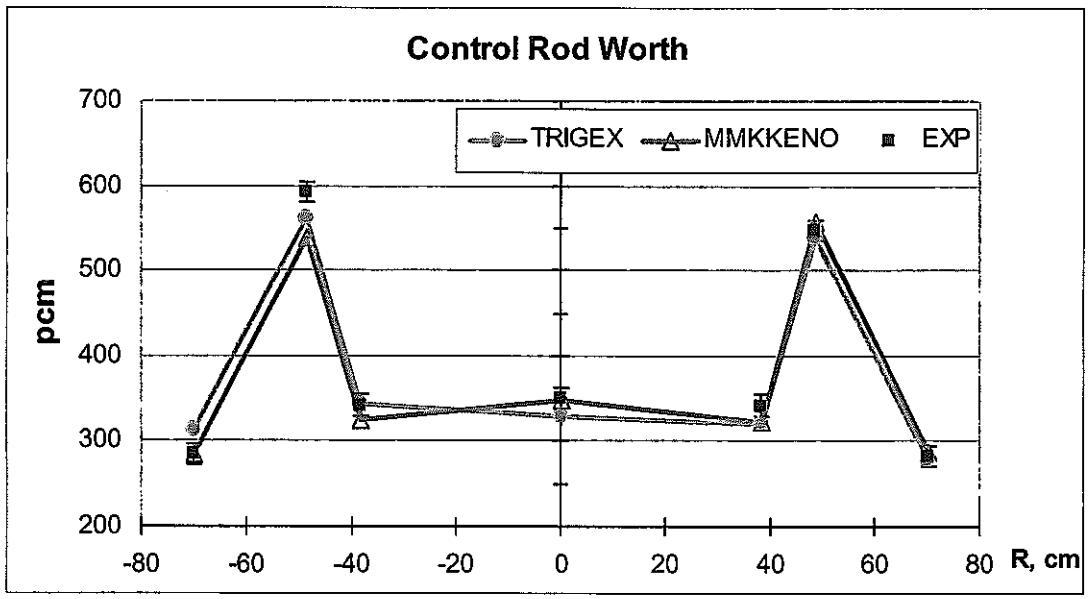

Fig. 11. Efficiency of the control rod mock-ups

3.5. Reaction Rate Distribution

3.5.1. Radial Direction

Distribution of uranium-235, uranium-238 and plutonium-239 fission reaction rates was measured by the small size fission chambers located in the inter-tube space at the level of the core midplane from core center to stainless steel reflector. Figure 12 shows location of measurement points. The uncertainty of measurement of fission rates of uranium-235 and plutonium-239 in the core and in the blanket is respectively 1.5-2% and 3-4%. For uranium-238, experimental error is some higher, namely: 2-3% within the core boundaries and 5-7% - in the blanket. Basic components of errors are uncertainty of exact location of the chambers, errors of its compositions and statistical error /14/.

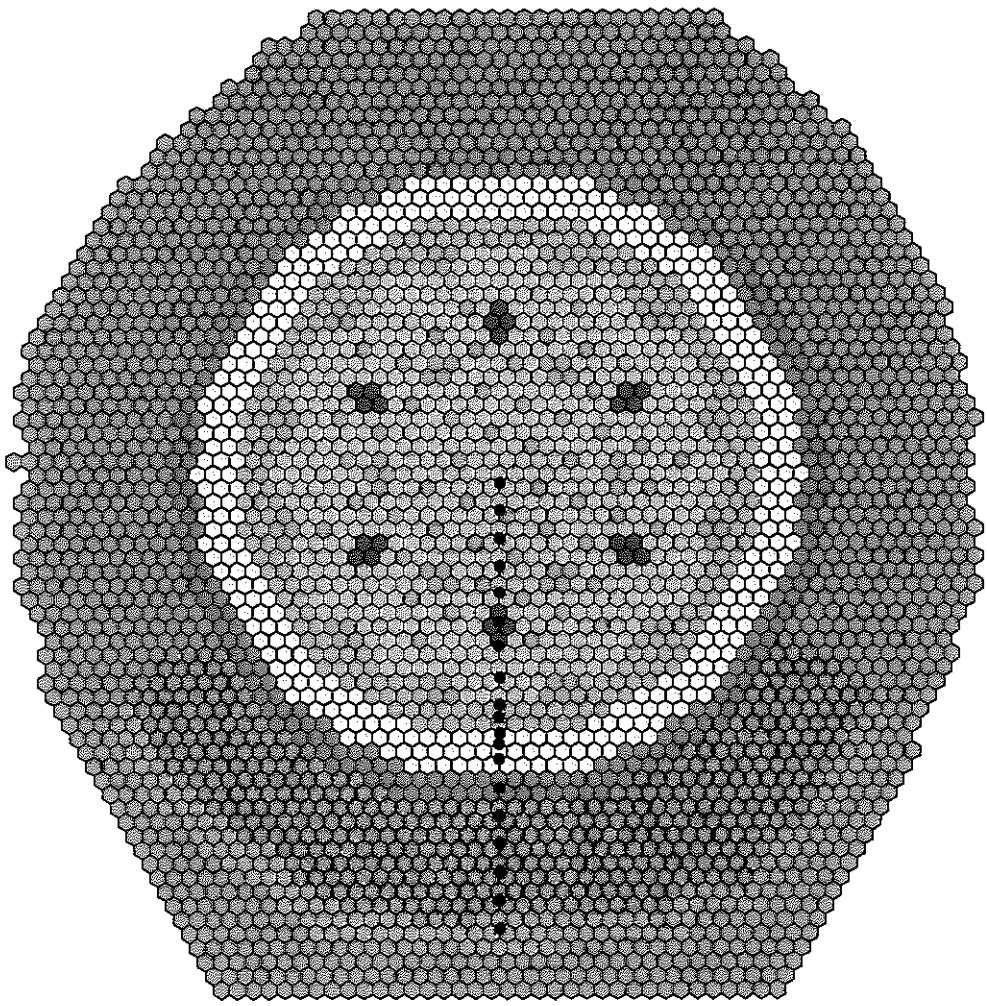

Fig. 12. Location of measurement points

These fission rate distributions have been calculated by TRIGEX in homogeneous approximation. Also transport and heterogeneous corrections were defined. Obtained results show that transport corrections are not great inside core. However these factors are necessary for SS reflector and for boron shield especially for U-238 fission rate distribution so it can change from 0.9 to 1.3 in this case.

Heterogeneous corrections were determined separately by using FFCP like:

$$K_{het} = \frac{\langle \sigma_{het} \rangle}{\sigma_{\text{hom}}} \qquad \text{where} \qquad \langle \sigma_{het} \rangle = \frac{\sum_{n=1}^{M} \overline{\sigma}_{x,i,n} \bullet F_n \bullet V_n}{\sum_{n=1}^{M} F_n \bullet V_n} \qquad (12);$$

$\langle \sigma_{het} \rangle$ were defined not over cell height but only over fission chamber height, i.e. 2 cm around core midplane.

For all cases calculation results were normalized on central core. Table 10 gives calculation results.

Table 10. Calculation results of the radial fission rate distributions

R, cm	Region	U-235	Pu-239	U-238
2.9	IC	1.001	1.002	0.995
11.8	IC	1.024	1.019	0.957
20.6	IC	1.019	1.018	0.957
29.5	IC	1.026	1.024	0.946
38.3	IC	1.048	1.043	0.923
47.1	SRF	1.141	1.137	0.774
55.9	IC	1.054	1.059	0.938
64.8	IC	0.995	1.024	1.043
73.6	MC	0.963	1.007	1.014
76.6	MC	0.948	0.992	1.001
82.4	MOX	0.896	0.949	1.114
85.4	MOX	0.859	0.915	1.149
91.3	MOX	0.776	0.829	1.064
100.1	OC	0.653	0.704	0.821
108.9	SSR	0.830	0.914	0.258
117.8	SSR	0.865	0.988	0.098
126.6	SSR	0.679	0.791	0.039
135.4	SSR	0.341	0.411	0.015
144.3	B_4C	0.050	0.049	0.006

3.5.2. Axial Direction

Special 2D R-Z model (see central part of this model on Fig. 13) has been created for these calculations on the base of "key region" model. Calculations were done in 28 groups S_8-transport and P_N approximations (TWODANT).

<table>
<tr><td>13.171</td><td rowspan="2">Axial Shield</td><td rowspan="2"></td><td rowspan="5">Empty Region</td><td rowspan="2">Axial Shield</td><td rowspan="2">Axial Shield</td><td>Empty Tube</td></tr>
<tr><td>26.689</td><td rowspan="3">A</td></tr>
<tr><td>23.021</td><td rowspan="2">Axial Blanket (pellets)*</td><td rowspan="3">Tube w/o sticks</td><td rowspan="2">Axial Blanket (pellets)**</td><td rowspan="2">Axial Blanket</td></tr>
<tr><td>6.369</td><td rowspan="4">F</td></tr>
<tr><td>103.81</td><td>IC
Laser (pellets)*</td><td>IC
Laser (pellets)**</td><td>IC
Laser</td></tr>
<tr><td>35.4</td><td>Axial Blanket (pellets)*</td><td>Axial Blanket (pellets)**</td><td>Axial Blanket</td></tr>
<tr><td>25.</td><td colspan="2">Support</td><td colspan="2">Support</td></tr>
<tr><td></td><td>2.34</td><td>0.16</td><td>0.18</td><td>10.</td><td>24.45</td><td>2.25</td></tr>
</table>

Fig. 13. Central part of the modified 2D R-Z model
(all sizes are given in cm)

Pellets* - pellets with cans only

Pellets** - pellets with cans and tube with sticks

Calculation points are placed inside "Empty Region". Total number of the calculation points is 251 (axial direction).

Calculation results are presented in Table 11.

Table 11. Calculation results of the axial fission rate distributions

H, cm	Region	U235-P3	PU239-P3	U238-TR	U238-P1	U238-P3
0.0		1.0000	1.0000	1.0000	1.0000	1.0000
2.5		0.9968	0.9961	0.9603	0.9750	0.9816
5.0		1.0187	1.0063	0.9226	0.9205	0.9268
7.5		0.9929	0.9864	0.9116	0.9176	0.9221
10.0		0.9654	0.9695	0.9518	0.9602	0.9677
12.5		0.9494	0.9557	0.9598	0.9513	0.9600
15.0		0.9187	0.9274	0.9022	0.9239	0.9290
17.5		0.9122	0.9172	0.9257	0.9143	0.9244
20.0	Core	0.8949	0.8973	0.8786	0.8873	0.8942
22.5		0.8922	0.8834	0.8093	0.8114	0.8164
25.0		0.8523	0.8475	0.7929	0.7925	0.7979
27.5		0.8088	0.8122	0.7914	0.8026	0.8084
30.0		0.7761	0.7806	0.7826	0.7750	0.7824
32.5		0.7323	0.7378	0.7203	0.7334	0.7385
35.0		0.7086	0.7103	0.7119	0.7030	0.7114
37.5		0.6781	0.6763	0.6554	0.6582	0.6646
40.0		0.6562	0.6447	0.5693	0.5724	0.5764
42.5		0.6103	0.6000	0.5405	0.5350	0.5408
45.0		0.5627	0.5562	0.5010	0.5101	0.5150
47.5		0.5309	0.5224	0.4598	0.4538	0.4598
50.0		0.4955	0.4849	0.3839	0.3885	0.3927
52.5		0.4933	0.4674	0.2785	0.2796	0.2804
55.0		0.4706	0.4401	0.2072	0.2123	0.2109
57.5		0.4448	0.4125	0.1575	0.1633	0.1613
60.0	Axial	0.4166	0.3847	0.1215	0.1269	0.1252
62.5	Blanket	0.3870	0.3573	0.0959	0.1002	0.0990
65.0		0.3582	0.3321	0.0759	0.0791	0.0784
67.5		0.3311	0.3099	0.0609	0.0633	0.0630
70.0		0.3073	0.2921	0.0485	0.0504	0.0504
72.5		0.2887	0.2805	0.0396	0.0408	0.0410
75.0		0.2760	0.2761	0.0321	0.0330	0.0333
77.5		0.2715	0.2813	0.0259	0.0266	0.0270
80.0		0.2795	0.3012	0.0205	0.0210	0.0214
82.5		0.3083	0.3507	0.0154	0.0157	0.0160
85.0		0.3290	0.3911	0.0118	0.0120	0.0123
87.5		0.3349	0.4119	0.0090	0.0091	0.0094
90.0	Shield	0.3293	0.4164	0.0070	0.0071	0.0074
92.5		0.3154	0.4080	0.0055	0.0055	0.0058

Table 11. Calculation results of the axial fission rate distributions (continued)

H, cm	Region	U235-P3	PU239-P3	U238-TR	U238-P1	U238-P3
95.0	Shield	0.2953	0.3896	0.0043	0.0042	0.0045
97.5		0.2713	0.3639	0.0033	0.0033	0.0035
100.0		0.2449	0.3330	0.0026	0.0025	0.0027
102.5		0.2172	0.2988	0.0020	0.0020	0.0021
105.0		0.1891	0.2626	0.0016	0.0015	0.0017
107.5		0.1611	0.2255	0.0012	0.0012	0.0013
110.0		0.1335	0.1882	0.0010	0.0009	0.0010
112.5		0.1066	0.1509	0.0007	0.0007	0.0008
115.0		0.0803	0.1139	0.0006	0.0005	0.0006
117.5		0.0544	0.0772	0.0004	0.0004	0.0004
120.0		0.0284	0.0402	0.0003	0.0003	0.0003

4. RELATIVE ANALYSIS OF CALCULATION AND EXPERIMENTAL RESULTS

4.1. Criticality and Spectral Indices

The results of comparison of calculation and experimental data on criticality are presented in Table 12.

Table 12. Comparison of experimental and calculation criticality values

	Code	k-eff
Base Monte-Carlo Result	MMKKENO	1.00163±0.00017 [a)]
Diffusion Result	TRIGEX	0.98689
Corrections		
Heterogeneity Effect	TRIGEX+FFCP	+0.0109±0.0020 [b)]
Transport Effect	TWODANT	+0.0043±0.0013 [b)]
Mesh Effect	TRIGEX	-0.0005±0.0003 [b)]
Model Effect	MMKKENO	-0.00135±0.00021 [a)]
Additional Heterogeneity	MMKKENO	+0.00212±0.00024 [a)]
Group Collapsing Effect	MMKKENO	-0.00054±0.00021 [a)]
Total Correction		+0.0149±0.0024
Corrected Result		1.0018±0.0024
Experiment		1.0007
C / E		***1.0011±0.0024***
C / E (Monte-Carlo)		***1.0009±0.0002***

[a)] statistical error

[b)] expert estimation /13/

The value of total heterogeneous effect obtained from Monte-Carlo calculations is +1.3%Δk/k (Chapter 3.1.1, Table 2). The value obtained by using TRIGEX+FFCP complex is close enough to this, however the latter result is slightly underestimation (0.2% approximately). It was proposed that this difference connected with approximations that put into the complex, i.e. 1-D modeling of real BFS cells with periodical boundary conditions, taken into account of heterogeneity only fuel cell etc. An

additional calculation was performed to check this assumption by using MMKKENO with "Simplified Heterogeneous Model" described above (Chapter 3.1.1). The criticality of simplified model was found on 0.21% lower than that for "as-built" model. This difference was named like "additional heterogeneity effect" and it should be considered under criticality evaluation.

The heterogeneous effect obtained by using TRIGEX+FFCP is agreed with MMKKENO result very well if "additional heterogeneity effect" will be taken into account.

The value of "model effect", i.e. adjusting of all axial layers and other model simplifications, shouldn't neglect under correct criticality estimation also. This effect has the opposite sign than the "additional heterogeneity effect" and practically compensates it in case BFS-62-3A assembly. However, the situation may be different when another critical assemblies will be under consideration.

Transport correction (correction for the diffusion approximation) is +0.43%Δk. Indirect confirmation of this value determined such non-traditional formula for very complicated configuration was obtained under comparison of two direct results – TRIGEX and Monte-Carlo. These calculations were done with the same homogeneous model and in 28-group approximation. The difference is equal 0.0045±0.0002 (taking into account statistical error).

The final result agrees well with the experiment. The rightness of accounting the corrections is confirmed by the agreement of TRIGEX calculation with the precise MMKKENO code calculation.

The results of comparison of calculation and experimental data on the spectral indices are given in Table 13. The calculation results on all indices agree well with the experimental data and the divergences are the same range of the experimental errors.

Table 13. Comparison of C/E values of the spectral indices

Index	C	E	C / E
F239/F235	0.9345	0.937±0.015	0.997±0.016
F238/F235	0.0207	0.0202±0.0004	1.025±0.020

4.2. Sodium Void Reactivity Effect

Special attention was paid to the study of the SVRE. The comparison of calculation and experimental results is given in pcm units in Table 14 and are illustrated on Fig. 14. The calculated β_{eff} value (TRIGEX code) was used to convert experimental data to pcm. β_{eff} is equal to 6.232^{-3}.

Table 14. Comparison of experimental and calculation SVRE values

Voided Core	C	E	C - E
Inner	-65.3	-57.3	-8.0
Middle	-15.0	-15.6	+0.6
MOX	-38.9	-32.4	-6.5
Outer	-62.4	-71.7	+9.3
TOTAL EFFECT	-181.6	-177.0	-4.6

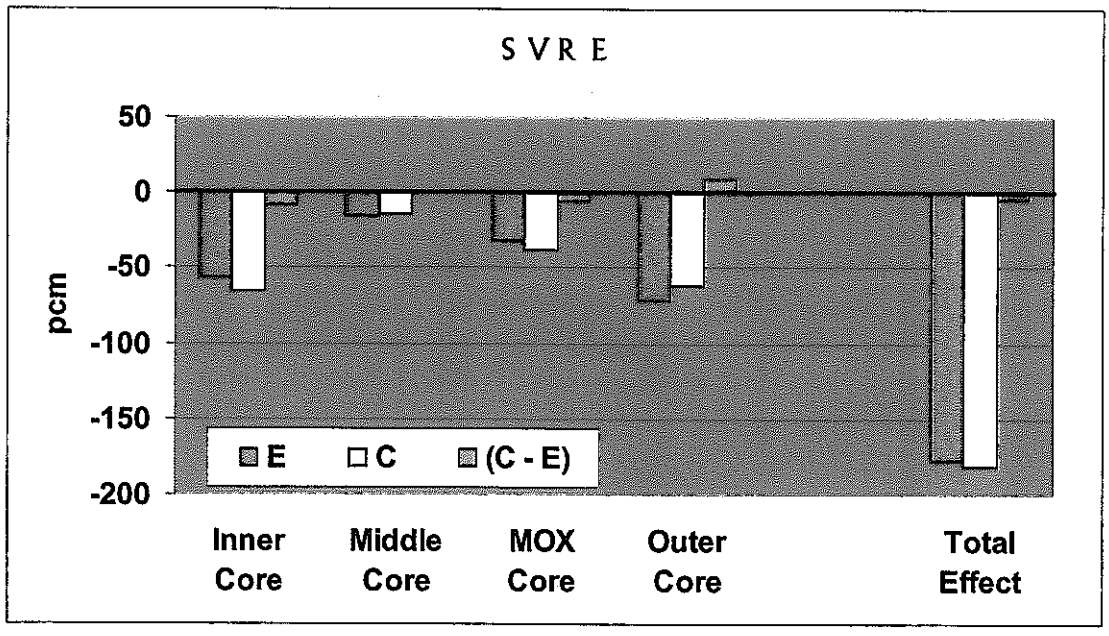

Fig. 14. SVRE. The Comparison of calculation and experimental results

There is some difference between experimental data and calculation results for region-wise SVRE, but these discrepancies are not systematical and (C-E) value isn't

larger than 5 pcm for total effect. If to extrapolate this value on whole core volume (multiplying by six), we will get the value ~30 pcm. It is essentially smaller than both cross-sections uncertainty and permissible error for this parameter which are estimated like 300 pcm approximately /16/.

It is accepted to consider that SVRE calculation error equals ±0.003 Δk/kk′ is permissible. From reactor safety consideration, an accident protection system is designed to be capable fully compensate positive reactivity effect under maximum core voiding condition. The analysis of calculation results of the international test /17/ have demonstrated that SVRE for fast reactor with MOX fuel and power ~800 MWt(e) is 2% Δk/kk′ /18,19/. Accident protection system for such reactor class is created with efficiency of not less than 3% Δk/kk′. Thus, assuming that possible error of efficiency estimation equals 10% (±0.003 Δk/kk′) and accepting the same value for SVRE it is possible to guarantee that reactor will be under criticality in case considered.

Such permissible error of SVRE is especially acceptable, when SVRE is negative.

4.3. Control Rod Worth

The results of calculation and experimental data comparison on control rod mock-up worth are given below in Table 15 and for clearness on Fig. 15. The calculation value of β_{eff} for the corresponding critical assembly conditions was used for such comparison.

Table 15. Comparison of C/E values of CRW

Type	Ring	Position	TRIGEX	MMKKENO
CR		Central	0.940	0.979
CR	1	3	1.003	0.948
CR	1	6	0.936	0.913
SR	2	2	0.948	0.881
SR	2	5	0.984	0.971
CR	3	5	1.095	0.994
CR	3	11	0.986	0.980
MEAN			**0.984**	**0.952**
St. Dev.			**0.055**	**0.041**

In this table, TRIGEX means deterministic corrected results and MMKKENO – homogeneous Monte-Carlo ones multiplied by heterogeneous correction factors (Table 8). In the whole, the discrepancies between two calculations and experiment did not exceed 6%, which can be assumed as a reasonable evaluation of the calculation accuracy.

Looking at Fig. 15, it should mark that in "key region" C/E values are very close between each other and difference lies inside statistical errors (fixed on the figure) of Monte-Carlo calculations. The discrepancies between calculation results for "green region" achieve 10%.

Perhaps, using of 3-D transport deterministic code may be useful for improving results in future, however the author has not such possibility now.

On the Fig. 15 positive direction points to stainless steel reflector and negative – to uranium blanket.

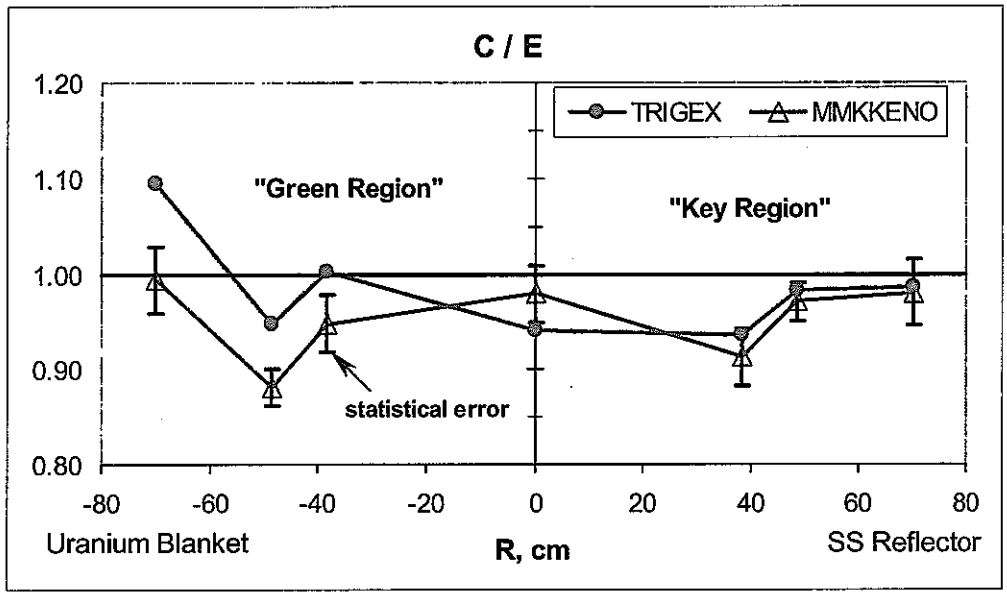

Fig. 15. C/E values for control rod worth

The efforts connected with definition of the control rod worth by the Monte-Carlo method with "as-built" model were not successful because there are big fluctuations and results are not stable after 20,000,000 histories yet (especially for outer ring CR).

Changing of the calculation reactivities from million to million histories with statistical errors and experimental data are presented on Fig. 16.

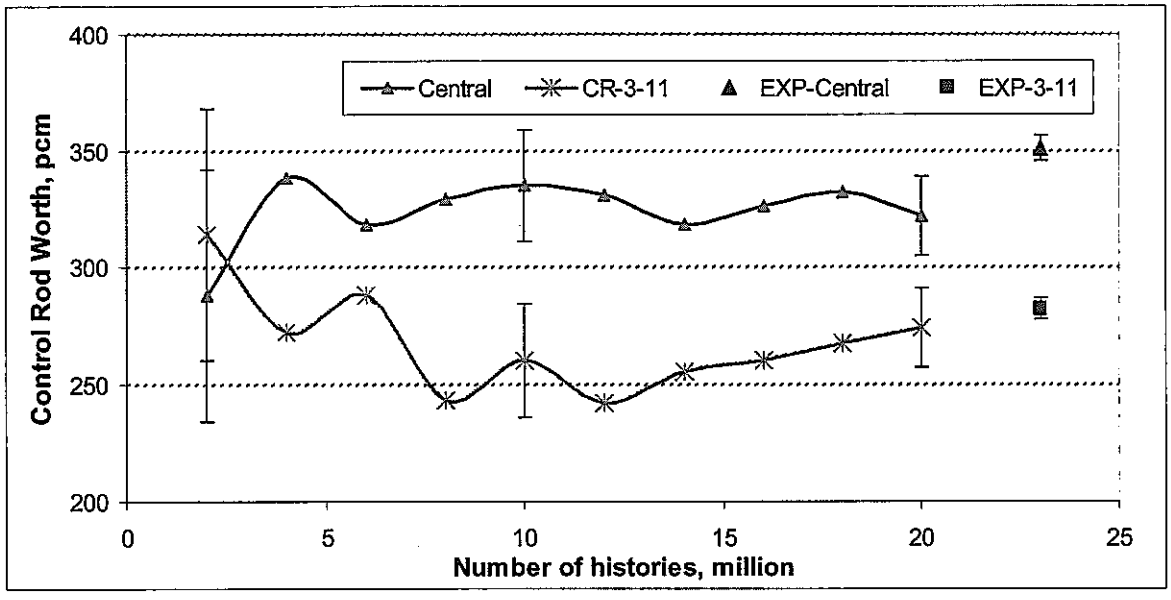

Fig. 16. CRW calculated for "As-Built" model

4.4. Reaction Rate Distribution

The results of calculation data comparison on fission rate distributions of uranium-235, plutonium-239 and uranium-238 are given at the presented below Figs. 17 and 18. One can mark the following. The maximal disagreements between the calculation and the experiment for uranium-235 and plutonium-239 fission rate in the volume of the core are about 4%. In the steel reflector the difference of calculation from the experiment in these reactions can achieve +20~+30%. Generally speaking, from the scientific point of view, the presence of such sizeable disagreements is interesting. However, from the practical point of view, it is not so essential because the power distribution in the steel blanket is determined not by these reactions, but mostly by gamma rays. Neither TRIGEX code is intended for performing such calculations and will not be verified for this purpose.

For a threshold uranium-238 fission reaction the scale of maximum disagreements is about ~5% - in the core and ~-30% in the outer layers of the steel reflector.

Comparison between experimental data and calculation results are presented in Tables 16, 17 and on Figures 17, 18.

Table 16. Comparison of C/E values of radial fission rate distributions

R, cm	Region	U-235	Pu-239	U-238
2.9	Inner	0.98	0.97	0.98
11.8	Inner	0.98	0.97	1.00
20.6	Inner	0.98	0.97	0.98
29.5	Inner	0.98	0.98	0.99
38.3	Inner	0.98	0.98	1.02
47.1	SR Follower	0.94	0.95	1.03
55.9	Inner	0.99	1.00	1.04
64.8	Inner	1.03	1.03	1.04
73.6	Middle	1.03	1.04	1.02
76.6	Middle	1.04	1.05	0.99
82.4	MOX	1.04	1.05	0.98
85.4	MOX	1.03	1.03	0.98
91.3	MOX	1.02	1.03	0.98
100.1	Outer	1.01	1.01	0.97
108.9	SS Reflector	1.12	1.17	0.91
117.8	SS Reflector	1.19	1.27	0.88
126.6	SS Reflector	1.21	1.32	0.83
135.4	SS Reflector	1.22	1.37	0.74
144.3	B_4C	0.93	0.97	0.73

For all cases calculation results in radial direction were normalized not on central point but on experimental and calculation integrals ratio inside core. This method of normalizing seems more reliable.

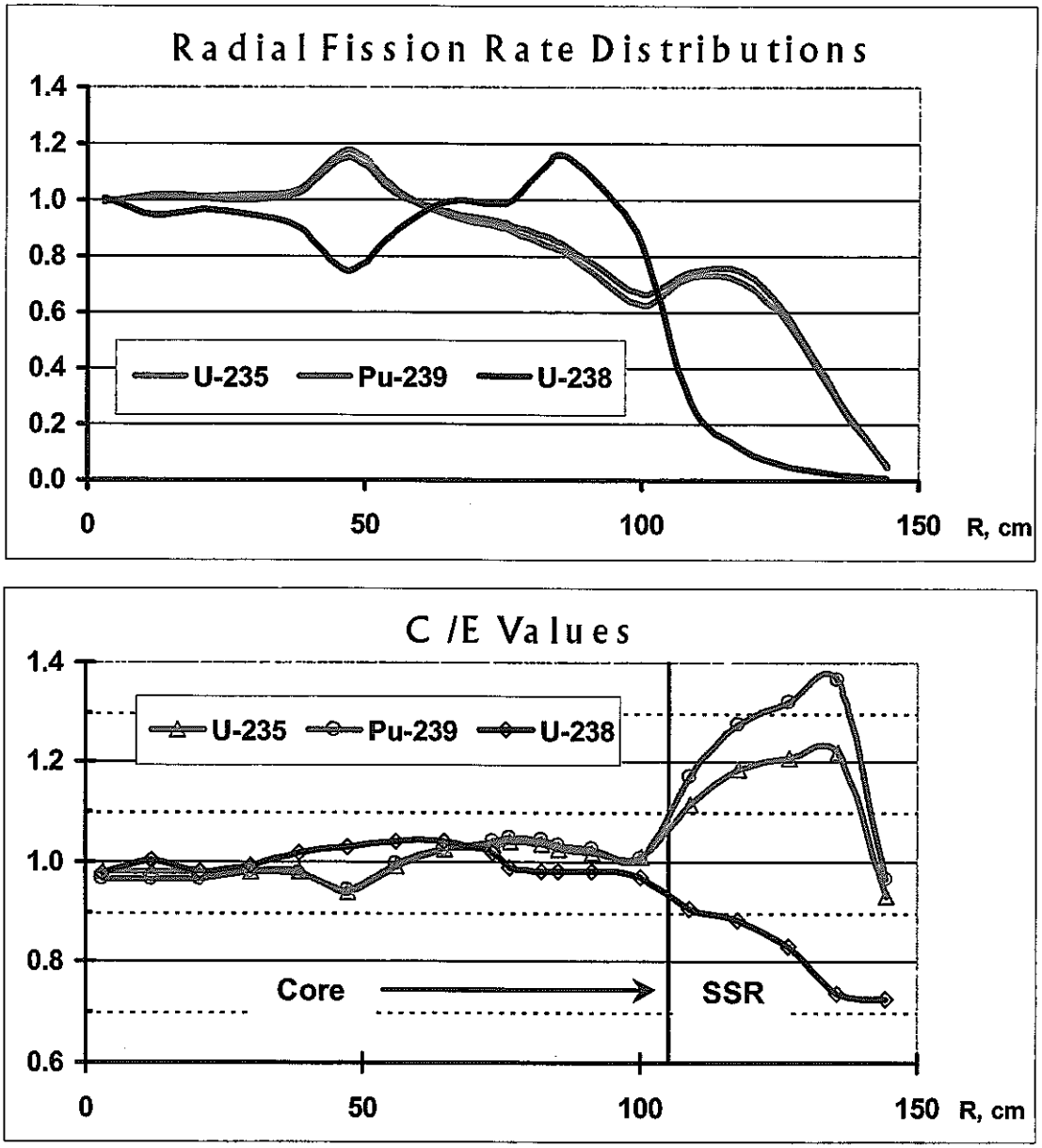

Fig. 17. Fission rate distributions and C/E values in radial direction

It was found that for U-238 fission rate distribution in axial direction the applying more higher P_N approximation leads to increasing results in compare with transport one.

Table 17. Comparison of C/E values of axial fission rate distributions

H, cm	U235-P3	PU239-P3	U238-TR	U238-P1	U238-P3
0.0	0.998	1.006	0.992	0.992	0.992
2.5	0.984	0.993	0.989	1.004	1.011
5.0	0.995	1.000	0.983	0.981	0.987
7.5	0.998	1.001	0.977	0.983	0.988
10.0	0.999	1.004	0.980	0.989	0.996
12.5	1.002	1.013	1.003	0.994	1.003
15.0	0.999	1.010	0.943	0.966	0.971
17.5	1.009	1.018	1.010	0.997	1.008
20.0	0.985	0.995	1.008	1.018	1.026
22.5	1.014	1.009	0.980	0.983	0.989
25.0	1.014	1.018	0.976	0.975	0.982
27.5	1.009	1.023	0.987	1.002	1.009
30.0	1.022	1.017	1.008	0.998	1.008
32.5	1.000	1.010	0.989	1.007	1.014
35.0	1.016	1.008	1.011	0.999	1.010
37.5	1.002	1.010	1.037	1.042	1.052
40.0	1.024	1.004	0.975	0.980	0.987
42.5	0.997	1.001	0.993	0.983	0.993
45.0	0.997	0.996	0.957	0.975	0.984
47.5	0.999	1.005	1.024	1.011	1.024
50.0	0.966	0.976	1.051	1.064	1.075
52.5	0.988	0.988	1.070	1.074	1.077
55.0	0.993	0.983	0.984	1.009	1.002
57.5	0.991	0.975	0.993	1.030	1.017
60.0	0.983	0.970	0.982	1.026	1.012
62.5	0.982	0.961	0.974	1.017	1.005
65.0	0.989	0.976	0.930	0.970	0.961
67.5	0.986	0.954	0.957	0.995	0.990
70.0	0.974	0.955	0.923	0.958	0.957
72.5	0.973	0.953	0.912	0.941	0.945
75.0	0.971	0.952	0.896	0.921	0.931
77.5	0.982	0.968	0.939	0.964	0.979
80.0	0.988	1.008	0.958	0.982	1.000
82.5	1.053	1.085	0.903	0.923	0.942
85.0	1.127	1.169	0.858	0.876	0.898

Table 17. Comparison of C/E values of axial fission rate distributions (continued)

H, cm	U235-P3	PU239-P3	U238-TR	U238-P1	U238-P3
87.5	1.176	1.230	0.831	0.845	0.872
90.0	1.197	1.256	0.829	0.833	0.867
92.5	1.206	1.224	1.021	1.024	1.071
95.0	1.225	1.217	0.839	0.832	0.879
97.5	1.217	1.182	0.896	0.880	0.939
100.0	1.196	1.151	0.836	0.814	0.877
102.5	1.252	1.239	0.777	0.750	0.815
105.0	1.283	1.277	0.689	0.656	0.719
107.5	1.261	1.256	0.730	0.691	0.763
110.0	1.255	1.262	0.686	0.641	0.715
112.5	1.250	1.298	0.669	0.618	0.696
115.0	1.272	1.319	0.801	0.734	0.833
117.5	1.201	1.248	0.847	0.770	0.879
120.0	0.847	0.829	0.969	0.881	1.013
Mean					
Core	**1.001**	**1.005**	**0.994**	**0.997**	**1.005**
Blanket	**0.983**	**0.970**	**0.960**	**0.990**	**0.990**
SS Shield	**1.212**	**1.228**	**0.814**	**0.793**	**0.851**

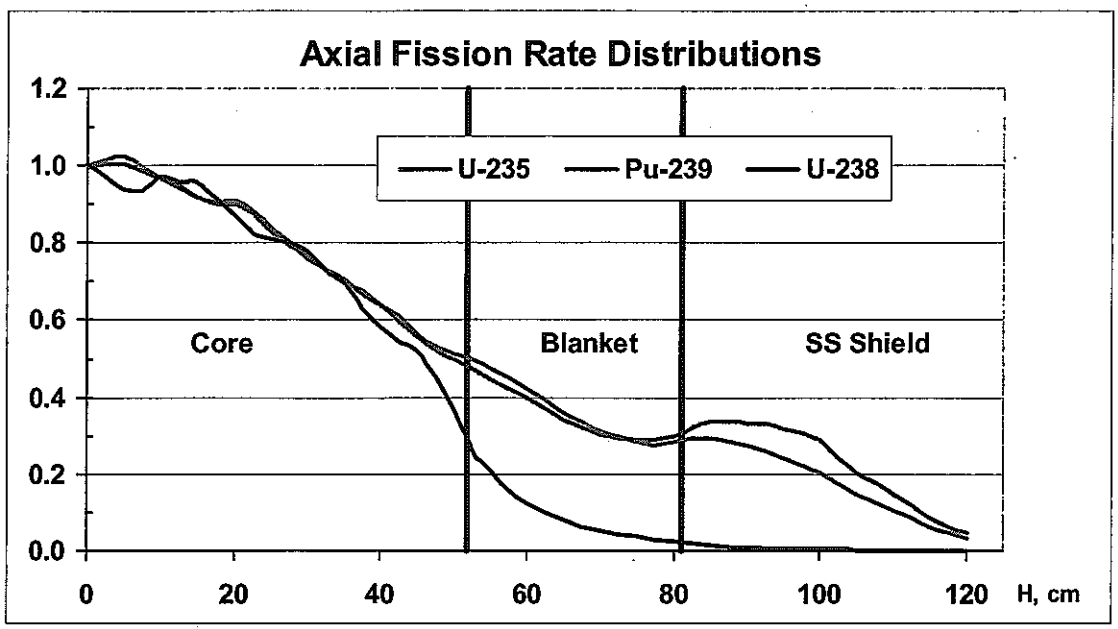

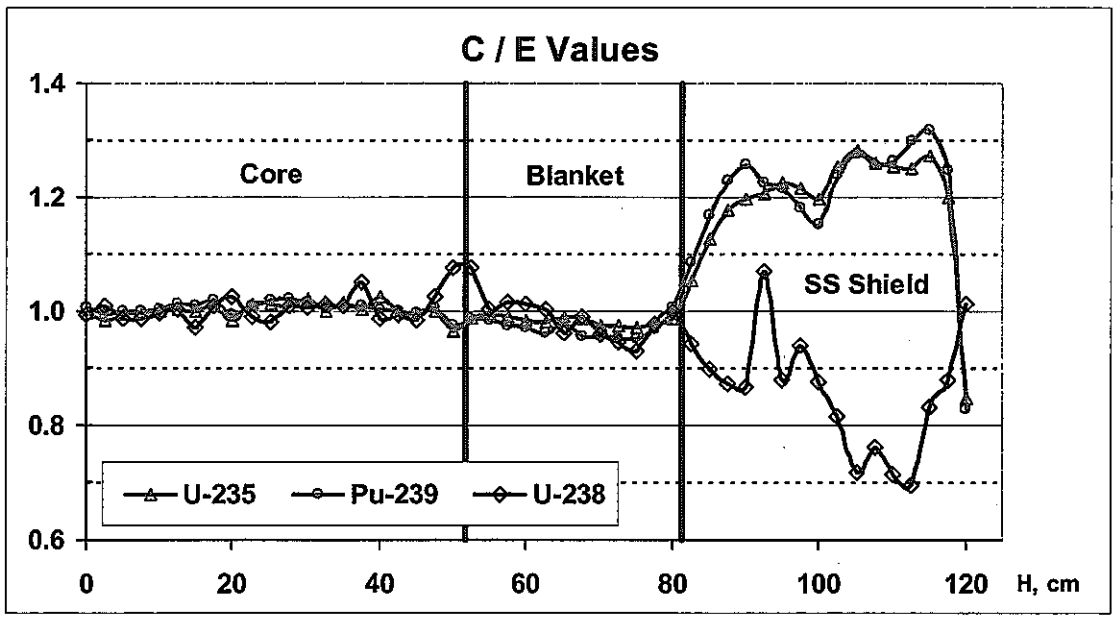

Fig. 18. Fission rate distributions and C/E values in axial direction

5. CONCLUSION

The given report presents a big volume of the analysis results on BFS-62-3A performed by Russian standard neutronics calculation codes.

The FFCP code considers the heterogeneity of the critical assembly and prepares the averaged cross-section set for diffusion calculation code TRIGEX to evaluate the corresponding heterogeneous correction.

The value of heterogeneous correction for the investigated assembly's criticality was +1.3%Δk/k. Transport correction (the diffusion approximation corrections) was evaluated as +0.4%Δk/k. Those correction values were confirmed by the precise Monte-Carlo calculations using the MMKKENO code.

Taking into account the mentioned corrections, disagreements between the calculation and experiment are within the following values:

- k_{eff} 0.1% Δk/k;
- Control rod worth 6%;
- SVRE 0.2 pcm/kg;
- Spectral indexes:
  - f8/f5 3%;
  - f9/f5 0.5%;
- Reaction rates:
- uranium-235 and plutonium-239 fission:
  - core 4%;
  - axial uranium blanket 4%;
  - steel reflector 20~30%;
- uranium-238 fission:
  - core 5%:
  - axial uranium blanket 7%;
  - steel reflector 20~30%.

The main result of this study is that the standard IPPE route with ABBN-93 nuclear cross-section set describes measured items well enough. Good agreement between the calculated and measurement values was confirmed on most parameters,

including criticality, spectral indices, SVRE and fission rate distribution in the core and blanket. The discrepancies for these items did not exceed experimental errors, as a rule.

The discrepancies for CRW are higher; however do not exceed 6%, which can be assumed as a reasonable evaluation of the calculation accuracy.

Furthermore, it should be noted that considerable inconsistency between the calculated and measurement values was found for the fission rate distribution in the stainless steel reflector region. From my point of view, the further investigations connected with improvement of nuclear data libraries for structural elements will be useful to resolve this problem.

It is supposed that those results can be effectively utilized for future investigation on analysis accuracy evaluation of the BN-600 hybrid core.

6. ACKNOWLEDGEMENTS

The author is very thankful to Mr. Akira Shono for the fruitful discussions and helpful comments.

REFERENCES

1. A.S. Seryogin, T.S.Kislitsyna, "Abstract of TRIGEX-CONSYST-ABBN-90", Preprint IPPE, 2655 (1997), (in Russian).

2. G.N. Manturov, M.N. Nikolaev, A.M. Tsiboulia, "ABBN-93 group constants system. Part 1: Nuclear Constants for Calculation of Neutron and Photon Radiation Fields", Issues of Nuclear Science and Technology, Series: Nuclear Constants, Vol. 1, p.59 (1996) , (in Russian).

3. A.A. Blyskavka, G.N. Manturov, M.N. Nikolaev, A.M. Tsiboulia, "Complex code CONSYST/MMKKENO to calculate nuclear reactors by the Monte-Carlo method in multigroup approximation with scattering indicatrix in P_n – approximation", Preprint IPPE, 2887 (2001), (in Russian).

4. RSICC COMPUTER CODE COLLECTION, "TWODANT-SYS. One- and Two-Dimentional, Multigroup, Discrete-Ordinates Transport Code System", ORNL.CCC-547, (1992).

5. G.N. Manturov, M.N. Nikolayev, A.M. Tsiboulia, "Code for Constants Preparation CONSYST", Preprint IPPE, 2857 (2000), (in Russian).

6. A.A. Bezbordov, B.G. Ryazanov, M.M. Savos'kin, "Evaluation of Heterogeneous Effects by Method of the First Collision Probability in Fast Neutron Critical Assemblies", Issues of Nuclear Science and Technology, Series: Physics and Technology of Nuclear Reactors, Vol. 2, p. 8 (1986), (in Russian).

7. ANISN, A One-Dimensional Discrete Ordinates Transport Code with Anisotropic Scattering. RSIC Computer Code Collection, CCC-254, ORNL.

8. A.Yu. Polyakov, A.A. Tsyboulya, "Independent Module FORAN in CONSYST System", Preprint IPPE, 2857 (2000), (in Russian).

9. RSIC PERIPHERAL SHIELDING ROUTINE COLLECTION AMPX-77, PSR-315, (1992).

10. RSIC COMPUTER CODE COLLECTION SCALE 4.3, "Modular Code System for Performing Standardized Computer Analyses for Licensing Evaluation for Workstations and Personal Computers", RSIC, ORNL, CCC-545, (rev.1996).

11. G. Bell, S. Glasstone, "Nuclear Reactor Theory", Krieger Publishing Company (1970).

12. J.L. Rowlands, "Physics of Fast Reactor Control Rods", Progress in Nuclear Energy, Vol. 16-3b, pp.287-321 (1985).

13. V. Dvuchsherstnov, et al., "Experimental and Calculation Studies Performed on BFS-62-3 Series", Preprint IPPE, 2853 (2000), (in Russian).

14. A. Kochetkov, I. Matveenko, V. Matveev, A. Tsiboulia, A. Shono, T. Hazama, M. Ishikawa, "BN-600 Hybrid Core Mock-Up at BFS-2 Critical Facility", PHYSOR 2002, Seoul, Korea, October 7-10 (2002).

15. A.S. Seryogin (IPPE), private communication (1996).

16. G.N. Manturov, V.I. Matveev, M.N. Nikolaev, M.F. Troyanov, A.M. Tsiboulia, "Accuracy Requirements for Calculation of Neutronics Characteristics of Fast Breeder Reactors: Degree and Ways of Its Satisfying", Atomnaya Energiya, Vol. 67, p. 181 (1989), (in Russian).

17. L.G. LeSage, R.D. McKnight, D.C. Wade, et al., "Proceedings of the NEACRP/IAEA Specialists Meeting on the International Comparison Calculation of a Large Sodium-cooled Fast Breeder Reactor", Argonne National Laboratory, Feb. 7-9, (1978), ANL-80-78, NEACRP-L-243, (1980).

18. G. Palmiootti, M. Salvatores, "NEACRP LMFBR Benchmark Calculation Intercomparison for Fuel Burnup", NEACRP-L-270, (1984).

19. M.Yu. Semenov, "The Analysis of Neutronics Experiments Performed on Fast Power Reactors for Checking and Substantiation of Group Cross-Sections Set", PhD Thesis, IPPE, Obninsk, (1998), (in Russian).

Appendix

BFS-62-3A. Homogeneous Nuclear Densities

Name	IC-L	IC-G	MC-L	MC-G	OC-L	OC-G	MOX-L	MOX-G
H	1.5820E-05	3.0062E-04	5.0247E-06	2.7626E-04	1.0623E-05	2.5474E-04	5.4267E-06	2.4954E-04
Na	6.5728E-03	6.5652E-03	6.2598E-03	6.2526E-03	5.6338E-03	5.6273E-03	5.6338E-03	5.6273E-03
C	3.0195E-04	3.0215E-04	4.0190E-04	4.0209E-04	3.6591E-04	3.6609E-04	4.2824E-04	4.2841E-04
AL	5.0196E-03	5.0204E-03	2.4161E-03	2.4169E-03	4.0036E-03	4.0043E-03	2.5889E-03	2.5895E-03
TI	1.1997E-04	1.2028E-04	1.3688E-04	1.3718E-04	1.3132E-04	1.3159E-04	1.3838E-04	1.3865E-04
CR	3.1507E-03	3.1591E-03	3.6349E-03	3.6429E-03	3.4462E-03	3.4534E-03	3.6993E-03	3.7065E-03
MN	2.4850E-04	2.4916E-04	2.8976E-04	2.9039E-04	2.7457E-04	2.7514E-04	2.9177E-04	2.9234E-04
FE	1.1429E-02	1.1459E-02	1.3168E-02	1.3196E-02	1.2513E-02	1.2539E-02	1.3410E-02	1.3436E-02
NI	1.4732E-03	1.4771E-03	1.7017E-03	1.7055E-03	1.6133E-03	1.6167E-03	1.7297E-03	1.7331E-03
U235	1.1876E-03	1.1876E-03	1.4786E-03	1.4786E-03	1.8646E-03	1.8646E-03	2.9720E-05	2.9720E-05
U238	6.7809E-03	6.7809E-03	6.7585E-03	6.7585E-03	7.0132E-03	7.0132E-03	7.1145E-03	7.1145E-03
O-16	1.3282E-02	1.3282E-02	1.3240E-02	1.3240E-02	1.4148E-02	1.4148E-02	1.4299E-02	1.4299E-02
B-10	-	-	-	-	-	-	-	-
B-11	-	-	-	-	-	-	-	-
PU239	-	-	-	-	-	-	1.4501E-03	1.4501E-03
PU240	-	-	-	-	-	-	7.0234E-05	7.0233E-05
PU241	-	-	-	-	-	-	8.0423E-07	8.0422E-07
AM241	-	-	-	-	-	-	2.9419E-06	2.9418E-06
GA	-	-	-	-	-	-	8.7691E-05	8.7690E-05

Name	W / F-L	W / F-G	IC-L (BR)	IC-G (BR)	OC-L (BR)	OC-G (BR)	RB	UAB-L
H	3.6178E-06	2.8842E-04	1.5820E-05	3.0062E-04	1.0623E-05	2.5474E-04	1.0700E-05	7.0993E-06
Na	6.5728E-03	6.5652E-03	6.5728E-03	6.5652E-03	5.6338E-03	5.6273E-03	-	5.5276E-03
C	3.0727E-04	3.0747E-04	3.0195E-04	3.0215E-04	3.6591E-04	3.6609E-04	6.9662E-04	4.9949E-04
AL	4.9902E-03	4.9910E-03	5.0196E-03	5.0204E-03	4.0036E-03	4.0043E-03	4.5454E-03	3.1570E-03
TI	1.2823E-04	1.2855E-04	1.1997E-04	1.2028E-04	1.3132E-04	1.3159E-04	4.3066E-05	8.6577E-05
CR	3.3718E-03	3.3802E-03	3.1507E-03	3.1591E-03	3.4462E-03	3.4534E-03	1.1513E-03	2.3146E-03
MN	2.6593E-04	2.6660E-04	2.4850E-04	2.4916E-04	2.7457E-04	2.7514E-04	9.0806E-05	1.8255E-04
FE	1.2196E-02	1.2227E-02	1.1467E-02	1.1497E-02	1.2513E-02	1.2539E-02	4.3813E-03	8.4758E-03
NI	1.5766E-03	1.5805E-03	1.4732E-03	1.4771E-03	1.6133E-03	1.6167E-03	5.3834E-04	1.0822E-03
U235	1.9814E-05	1.9814E-05	1.2222E-03	1.2222E-03	1.8610E-03	1.8610E-03	5.8599E-05	3.8880E-05
U238	4.7430E-03	4.7430E-03	6.8447E-03	6.8447E-03	7.0090E-03	7.0091E-03	1.4028E-02	9.3072E-03
O-16	1.2502E-02	1.2502E-02	1.3282E-02	1.3282E-02	1.4148E-02	1.4148E-02	2.8194E-02	1.8706E-02
B-10	-	-	-	-	-	-	-	-
B-11	-	-	-	-	-	-	-	-
PU239	-	-	-	-	-	-	-	-
PU240	-	-	-	-	-	-	-	-
PU241	-	-	-	-	-	-	-	-
AM241	-	-	-	-	-	-	-	-
GA	-	-	-	-	-	-	-	-

Name	LAB-G	UAB-G	FOLL-L	FOLL-G	ABS-L	ABS-G	B4C	UAS
H	2.4569E-04	2.4661E-04	-	4.7386E-04	-	4.2482E-04	-	3.5320E-04
Na	5.5007E-03	5.5213E-03	1.0936E-02	1.0924E-02	9.8043E-03	9.7931E-03	-	8.1420E-03
C	4.9780E-04	4.9966E-04	1.6468E-04	1.6501E-04	6.0934E-03	6.0937E-03	1.5003E-02	2.0820E-04
AL	3.1458E-03	3.1576E-03	6.2311E-04	6.2438E-04	2.4029E-04	2.4144E-04	1.7229E-04	7.8779E-04
TI	8.6518E-05	8.6842E-05	2.5612E-04	2.5665E-04	9.8771E-05	9.9241E-05	7.0817E-05	3.2381E-04
CR	2.3130E-03	2.3216E-03	6.8472E-03	6.8612E-03	2.6405E-03	2.6531E-03	1.8932E-03	8.6569E-03
MN	1.8243E-04	1.8311E-04	5.4004E-04	5.4115E-04	2.0826E-04	2.0925E-04	1.4932E-04	6.8278E-04
FE	8.4695E-03	8.5012E-03	2.4590E-02	2.4640E-02	9.4828E-03	9.5280E-03	6.7990E-03	3.1089E-02
NI	1.0815E-03	1.0856E-03	3.2016E-03	3.2082E-03	1.2347E-03	1.2405E-03	8.8523E-04	4.0478E-03
U235	3.8735E-05	3.8880E-05	-	-	-	-	-	-
U238	9.2725E-03	9.3072E-03	-	-	-	-	-	-
O-16	1.8636E-02	1.8706E-02	-	-	-	-	-	-
B-10	-	-	-	-	4.8000E-03	4.8000E-03	1.1907E-02	-
B-11	-	-	-	-	1.9320E-02	1.9320E-02	4.7925E-02	-
PU239	-	-	-	-	-	-	-	-
PU240	-	-	-	-	-	-	-	-
PU241	-	-	-	-	-	-	-	-
AM241	-	-	-	-	-	-	-	-
GA	-	-	-	-	-	-	-	-

Name	SUPPORT	SS REFL	B_4C (P)-1	B_4C (P)-2	TUBE+2St	TUBE
H	-	-	-	-	-	-
Na	-	-	-	-	-	-
C	9.2259E-05	2.4180E-04	1.0892E-02	1.1414E-02	4.5532E-05	2.7690E-05
AL	3.4909E-04	9.1493E-04	1.0477E-04	1.0477E-04	1.7229E-04	1.0477E-04
TI	1.4349E-04	3.7607E-04	4.3066E-05	4.3066E-05	7.0817E-05	4.3066E-05
CR	3.8361E-03	1.0054E-02	1.1513E-03	1.1513E-03	1.8932E-03	1.1513E-03
MN	3.0256E-04	7.9296E-04	9.0806E-05	9.0806E-05	1.4932E-04	9.0806E-05
FE	1.3776E-02	3.6106E-02	4.1347E-03	4.1347E-03	6.7990E-03	4.1347E-03
NI	1.7937E-03	4.7010E-03	5.3834E-04	5.3834E-04	8.8523E-04	5.3834E-04
U235	-	-	-	-	-	-
U238	-	-	-	-	-	-
O-16	-	-	-	-	-	-
B-10	-	-	8.6478E-03	9.0632E-03	-	-
B-11	-	-	3.4810E-02	3.6481E-02	-	-
PU239	-	-	-	-	-	-
PU240	-	-	-	-	-	-
PU241	-	-	-	-	-	-
AM241	-	-	-	-	-	-
GA	-	-	-	-	-	-